NASA CONTRACTOR REPORT

NASA CR-2714

LANDING GEAR AND CAVITY NOISE PREDICTION

Donald B. Bliss and Richard E. Hayden

Prepared by
BOLT BERANEK AND NEWMAN INC.
Cambridge, Mass. 02138
for Langley Research Center

NATIONAL AERONAUTICS AND SPACE ADMINISTRATION • WASHINGTON, D. C. • JULY 1976

1. Report No.	2. Government Accession No.	3. Recipient's Catalog No.
NASA CR-2714		

4. Title and Subtitle	5. Report Date
Landing Gear and Cavity Noise Prediction	July 1976
	6. Performing Organization Code

7. Author(s)	8. Performing Organization Report No.
Donald B. Bliss and Richard E. Hayden	
	10. Work Unit No. 505-06-23-01

9. Performing Organization Name and Address	11. Contract or Grant No.
Bolt Beranek and Newman Inc. 50 Moulton St. Cambridge, Mass. 02138	L18051A
	13. Type of Report and Period Covered
12. Sponsoring Agency Name and Address	Contractor Report
National Aeronautics & Space Administration Washington, DC 20546	14. Sponsoring Agency Code

15. Supplementary Notes

Langley technical monitor: Jay C. Hardin

16. Abstract

This paper is concerned with prediction of airframe noise radiation from the landing gear and wheel wells of commercial aircraft. Measurements of these components on typical aircraft are presented and potential noise sources identified. Semiempirical expressions for the sound generation by these sources are developed from available experimental data and theoretical analyses. These expressions are employed to estimate the noise radiation from the landing gear and wheel wells for a typical aircraft and to rank order the component sources.

17. Key Words (Suggested by Author(s))	18. Distribution Statement
Airframe Noise, Component Sources	Unclassified - Unlimited Subject Category 71

19. Security Classif. (of this report)	20. Security Classif. (of this page)	21. No. of Pages	22. Price*
Unclassified	Unclassified	56	$4.25

* For sale by the National Technical Information Service, Springfield, Virginia 22161

TABLE OF CONTENTS

LIST OF FIGURES AND TABLES

LIST OF FIGURES AND TABLES *(Cont.)*

LANDING GEAR AND CAVITY NOISE PREDICTION

By Donald B. Bliss and Richard E. Hayden
Bolt Beranek and Newman Inc.

INTRODUCTION

Airframe (nonpropulsive) noise is presently of concern since it represents a potential barrier to successful implementation of proposed noise regulations on commercial aircraft. In particular, the most commonly accepted future noise regulations are thought to be 10 PNdB below Federal Air Regulation 36 (FAR-36). Meeting this so-called FAR 36-10 criterion cannot be achieved by treating propulsion sources alone if airframe noise sources are at or above the FAR 36-10 dB level. Thus, it is important to identify the aircraft components and noise mechanisms responsible for airframe noise radiation and to attempt to predict the component noise levels.

Troublesome airframe noise occurs during the approach phase of flight, when power settings are relatively low and the aircraft is in a high lift, high drag configuration by virtue of deployment of flaps, slots, and landing gear and the presence of open cavities. The present work is confined to the effect of landing gear and cavities only. A broader treatment of the problem can be found in Hayden *et al.* (1974 and 1975) and Hardin *et al.* (1975).

Since typical glide slopes for CTOL aircraft are 3° from horizontal, the aircraft fly at low altitude for a long distance, thus potentially exposing a large area to noise. Before considering the landing gear/cavity noise mechanisms and predictions in detail, it is instructive to review the typical sequence of events undertaken by an aircraft preparatory to landing, since the airframe component configuration, airspeed, and altitude all play a role in the observed airframe noise, and all vary significantly during an approach. Figure 1 shows a typical sequence of flap and gear deployment as a function of distance from the airport along with the respective altitudes and airspeeds for CTOL jets in the current commercial fleet.

Reduced speed and increased flap angle characterize the early stages of final approach, which may begin 16 km (10 miles) from the touchdown point. At altitudes of 460 to 550 m (approximately 1500 to 1800 ft), the 3° glide slope is intercepted and the landing gear is deployed, involving the opening of various doors in the fuselage and wing. On many aircraft, some of the doors will reclose shortly after the gear deployment. When the

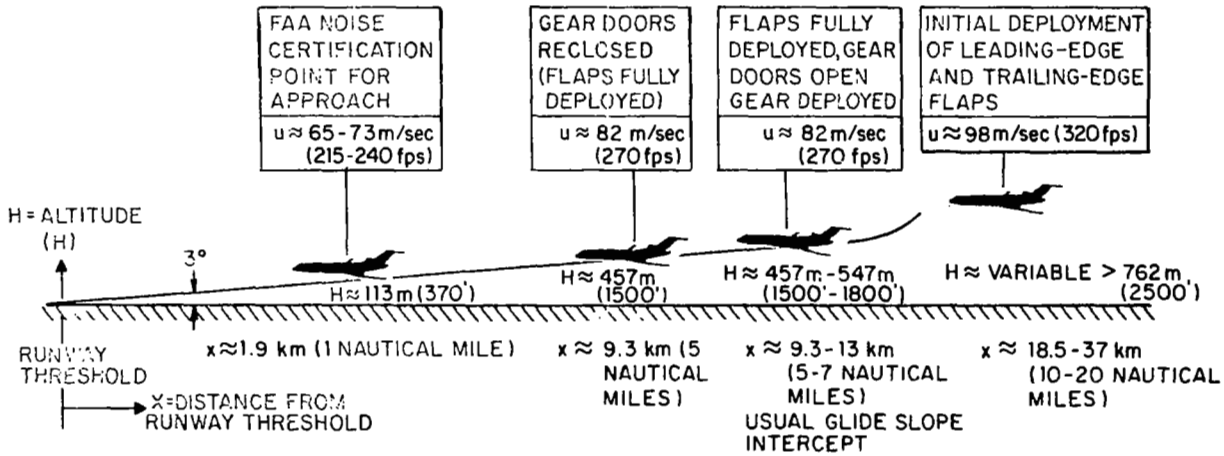

FIG. 1. TYPICAL SEQUENCE OF GEAR AND FLAP DEPLOYMENT.

aircraft crosses the FAA noise certification point, 1.85 km (1 nautical mile) from the threshold, it is traveling 66 to 73 m/sec (215 to 240 ft/sec) at an altitude of 113 m (370 ft). The noise is measured on a direct flyover. The allowable levels for aircraft noise are a function of aircraft gross weight. The typical components of concern are pointed out in Fig. 2 for a typical modern aircraft.

The details of flap geometry, setting angle, landing gear arrangement, and exact airspeed vary between aircraft types, and even between different aircraft of the same type, due to load factors, weather, traffic, and pilot techniques.

The following list is believed to include all the major contributors to airframe noise:

- Wings and stabilizers,
- Flaps,
- Landing gear "self-noise,"
- Landing gear cavity (wheel well) oscillations,
- Separated flow interaction of edges of cavities,
- Doors associated with gear deployment,
- Interaction of gear and cavity wakes with trailing edges and flaps.

In practice, one finds various configurations of flaps, e.g., one-, two-, or three-flap systems, leading-edge devices, and landing gear (single carriage, multiple carriage, in-line struts, etc.). The component noise prediction method enables one to account for the differences between configurations; this method may be important in determining and reducing the overall noise signature of the aircraft.

TYPICAL CONFIGURATIONS

In order to determine the gross geometry and characteristics of typical landing gear configurations, measurements and photographs were made of a Boeing 727 and a McDonnell-Douglas DC-9 (see Figs. 2 through 7). The landing gear arrangement in both aircraft is seen to be quite similar. Since the measurements were made on actual service aircraft, and not taken from detailed engineering drawings, the information given must be viewed as approximate. It is, however, quite adequate for present purposes.

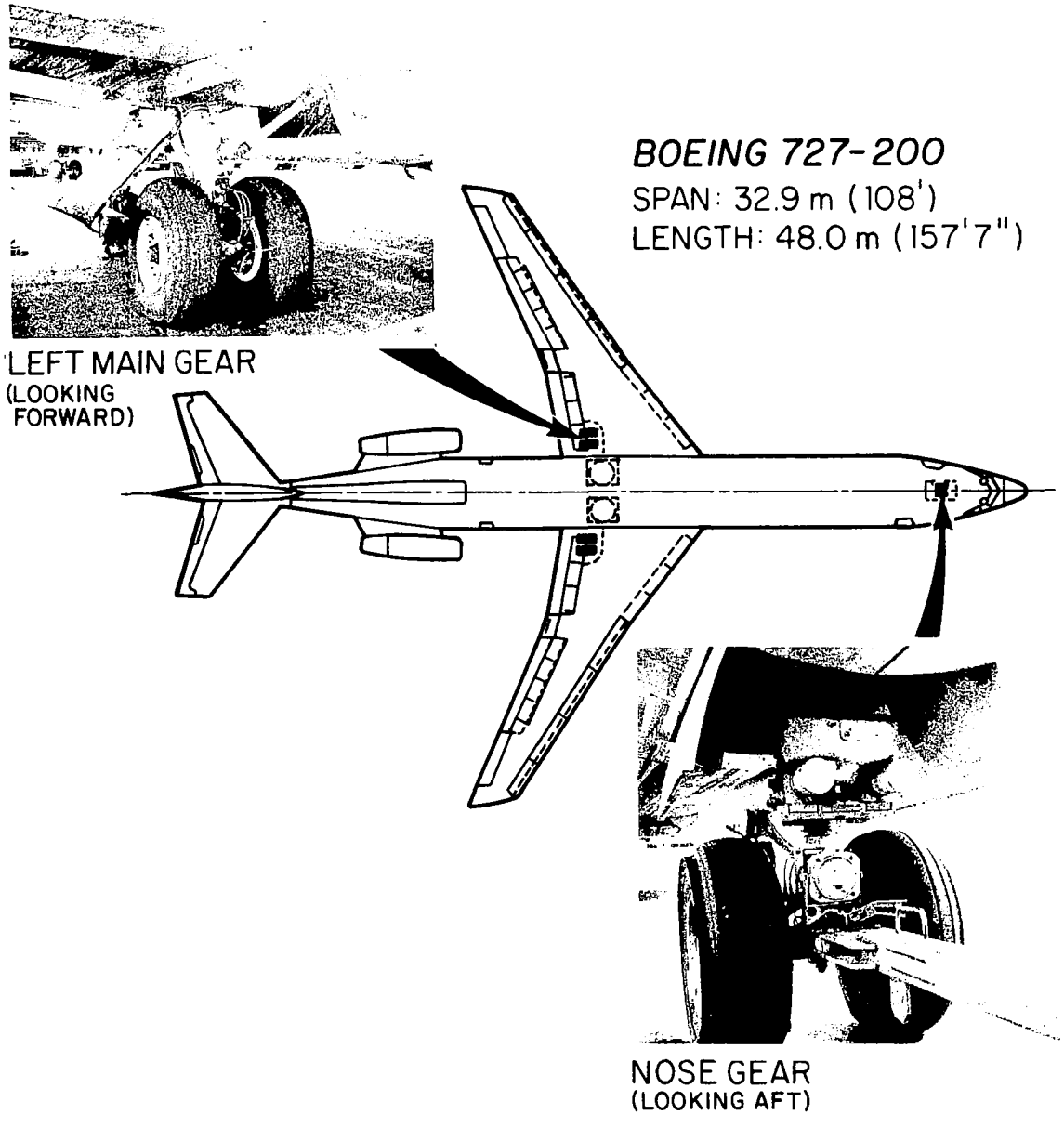

FIG. 2. EXAMPLE AIRCRAFT FOR LANDING GEAR/CAVITY NOISE CALCULATIONS.

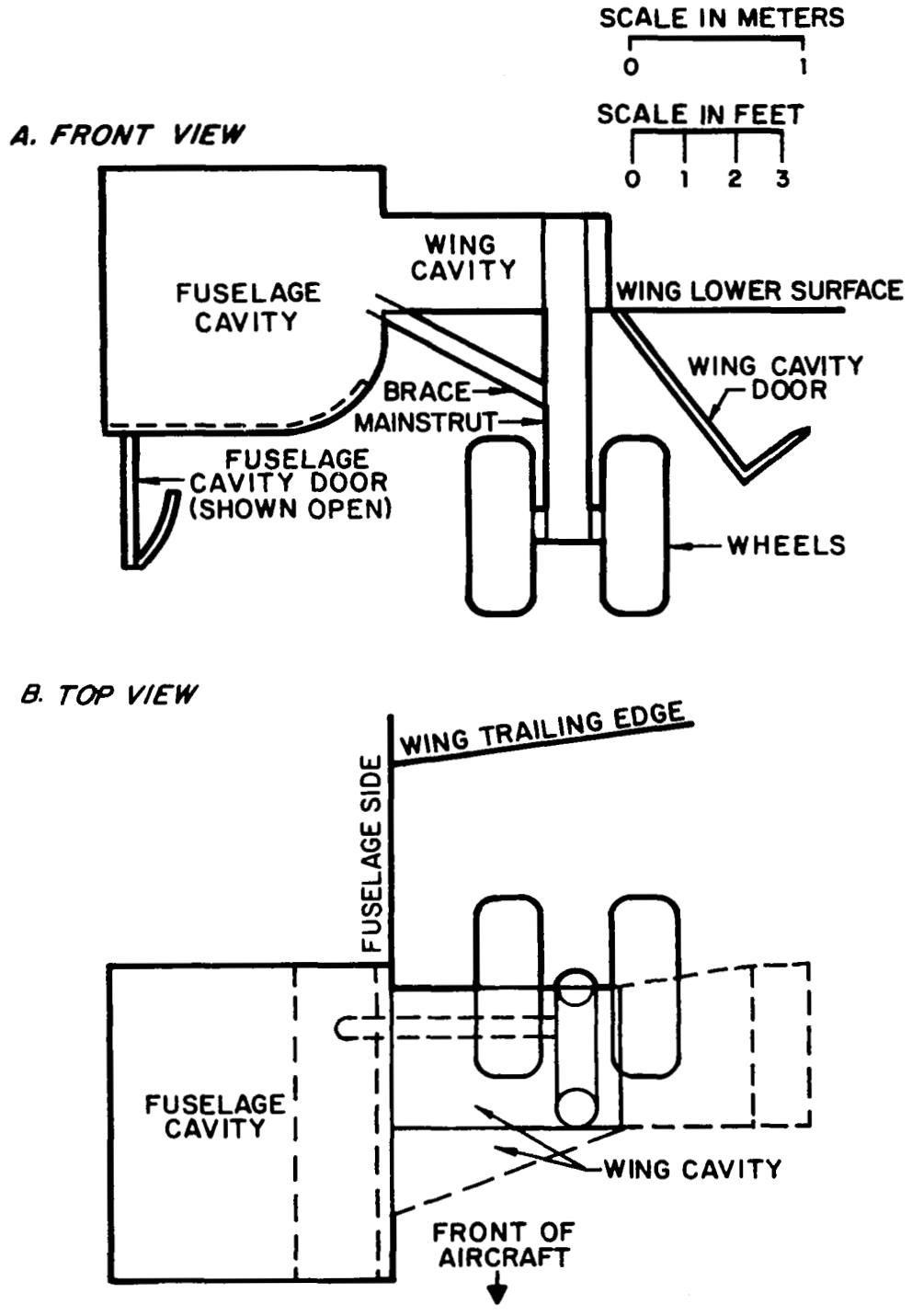

FIG. 3. BOEING 727 MAIN LANDING GEAR - Continued.

C. SIDE VIEW

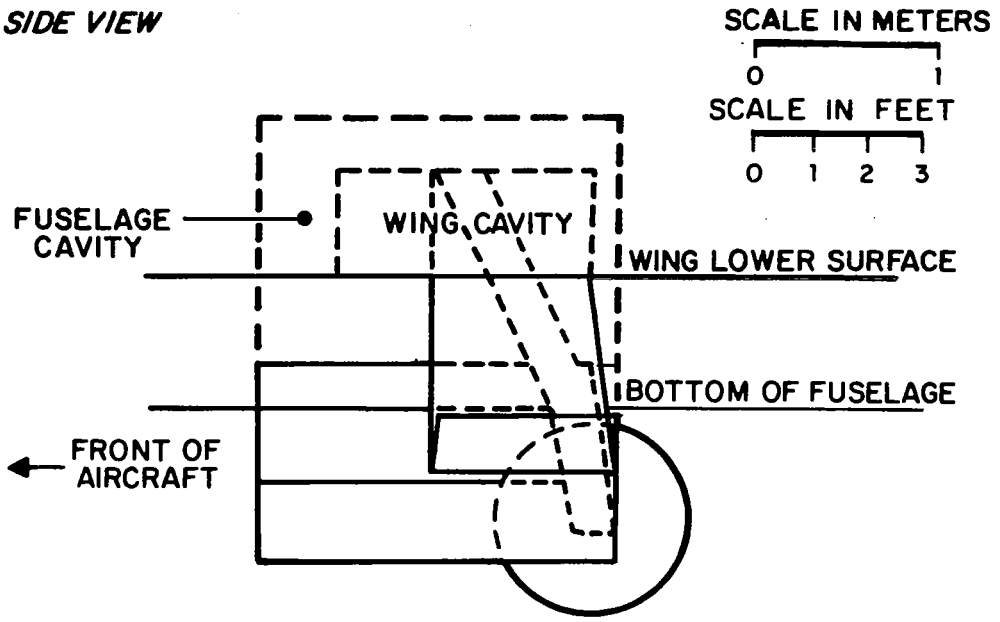

D. FUSELAGE CAVITY DETAIL

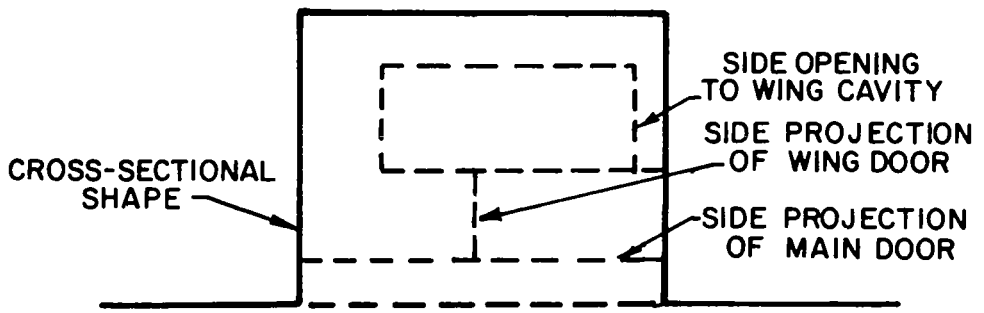

E. WING CAVITY DETAIL

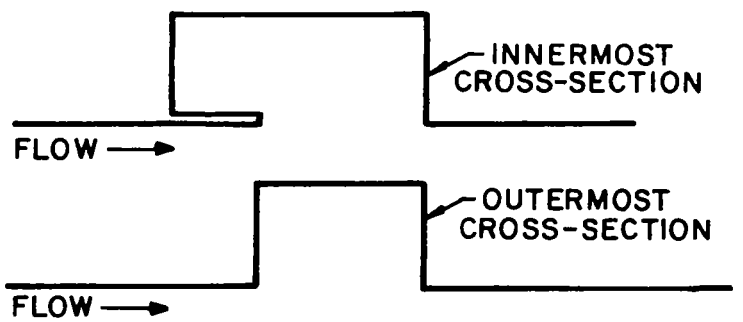

FIG. 3. BOEING 727 MAIN LANDING GEAR - Concluded.

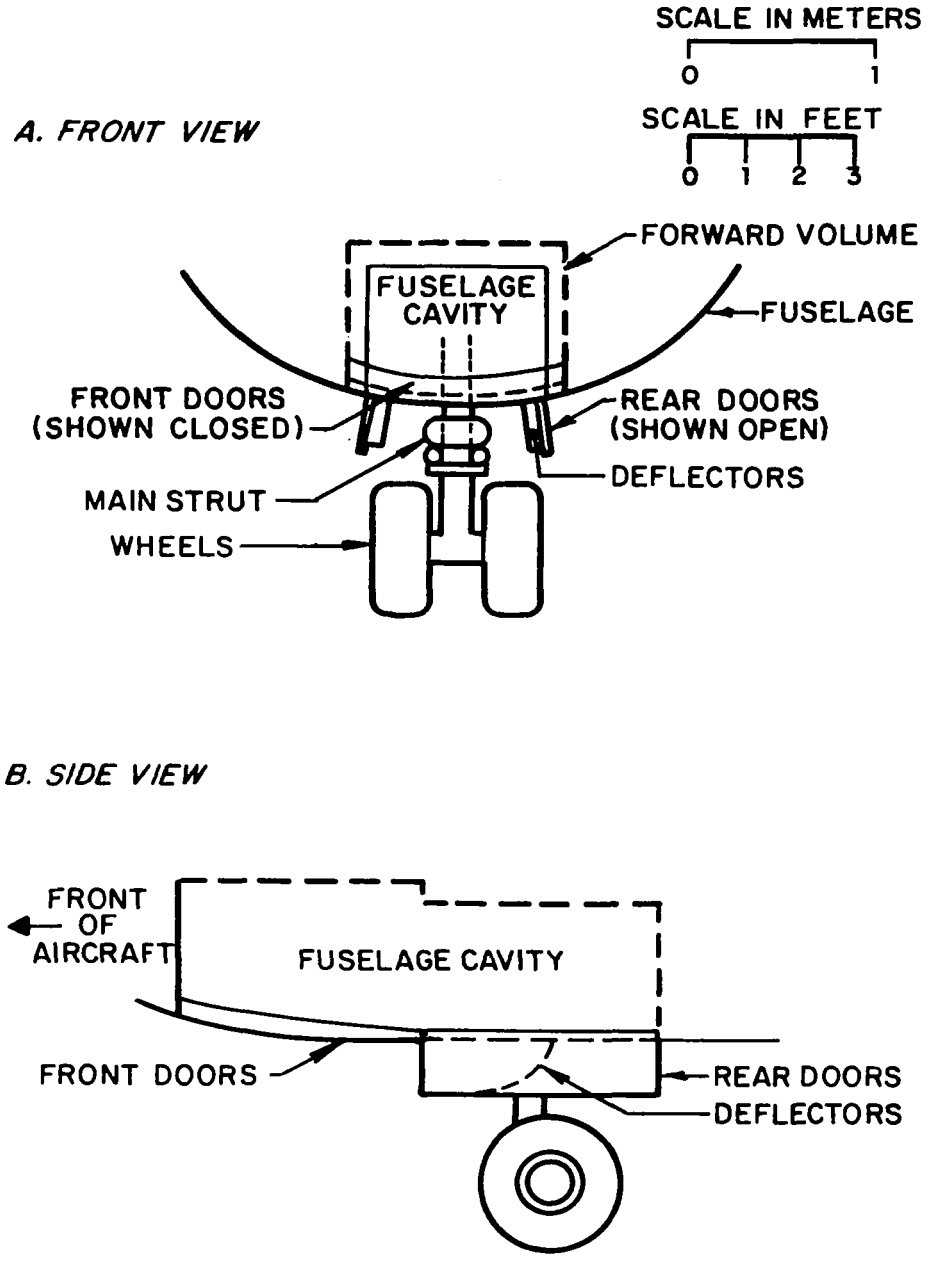

FIG. 4. BOEING 727 NOSE LANDING GEAR.

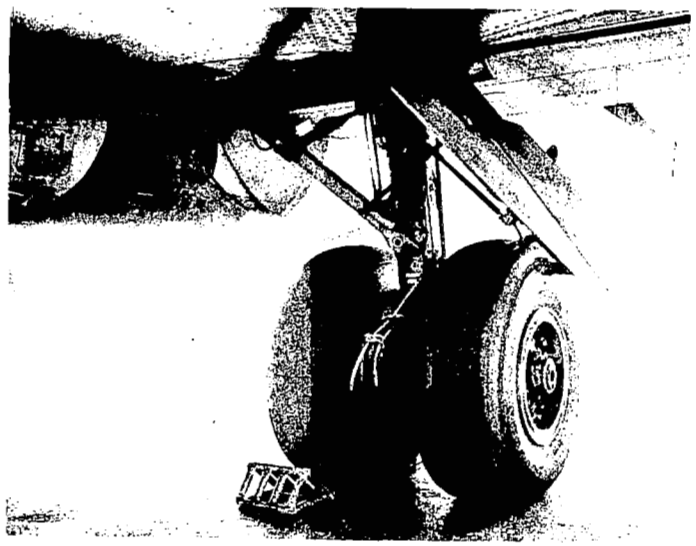

Main Gear Approach Condition as Seen from the Front

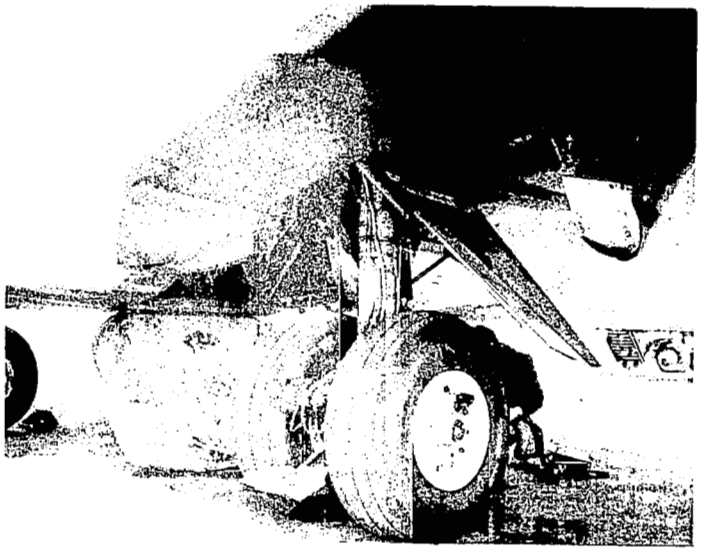

Main Gear with Fuselage Doors Open as Seen from Behind

FIG. 5. MCDONNELL-DOUGLAS DC-9 LANDING GEAR.

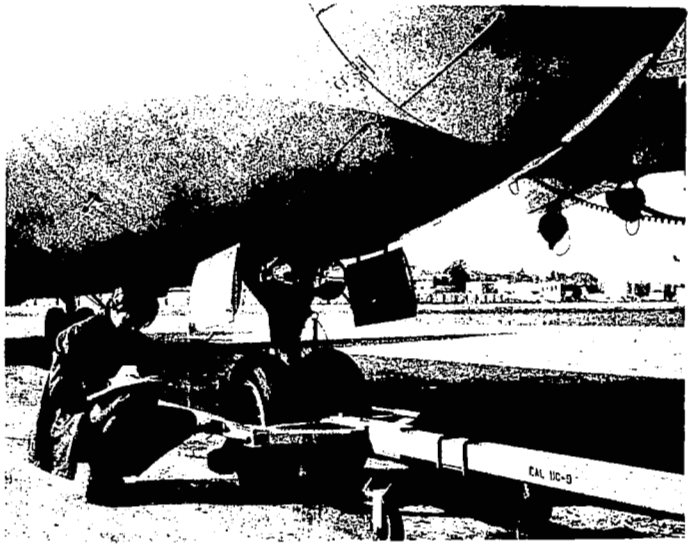

Nose Gear

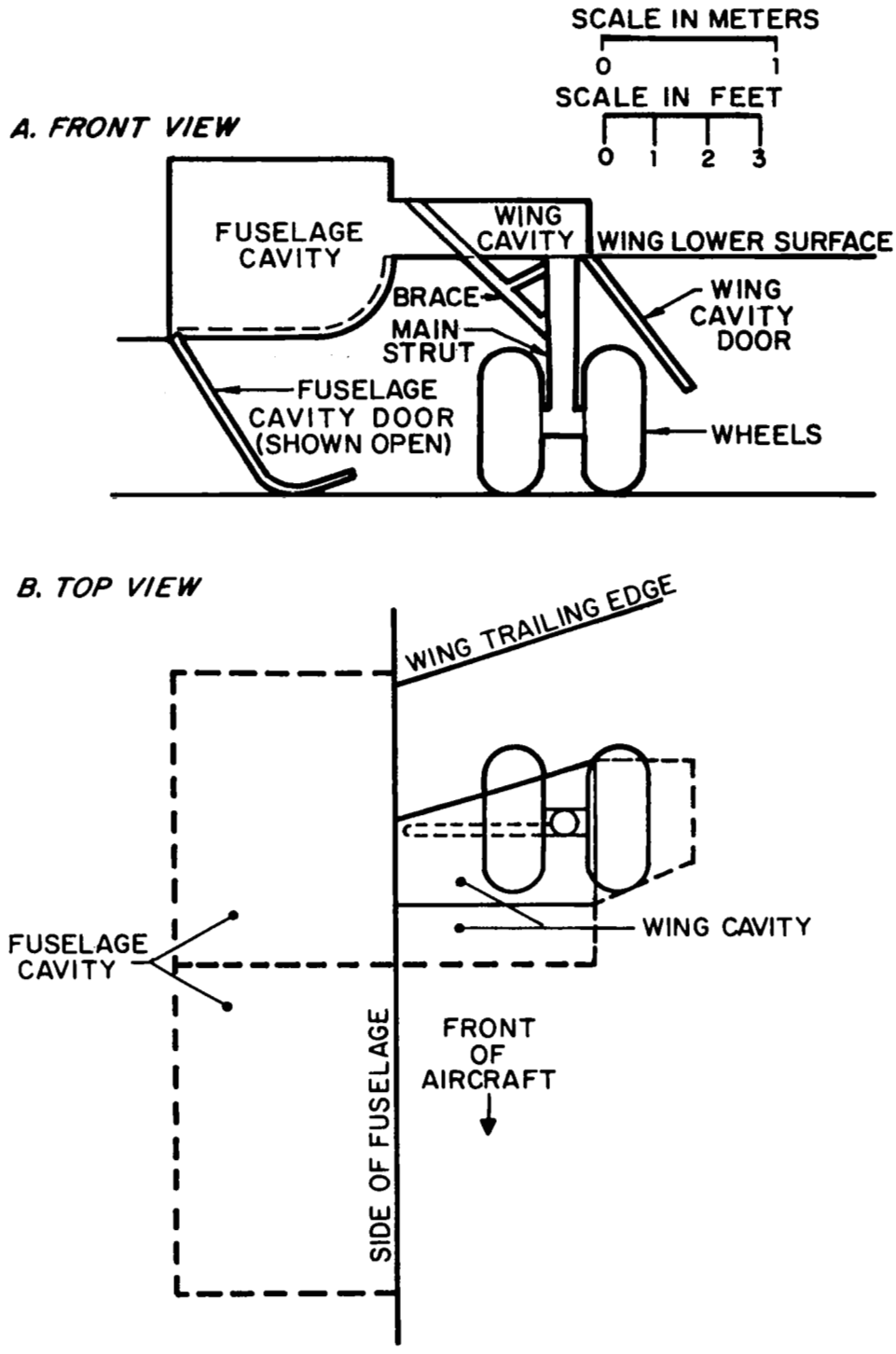

FIG. 6. MCDONNELL-DOUGLAS DC-9 MAIN LANDING GEAR (Continued).

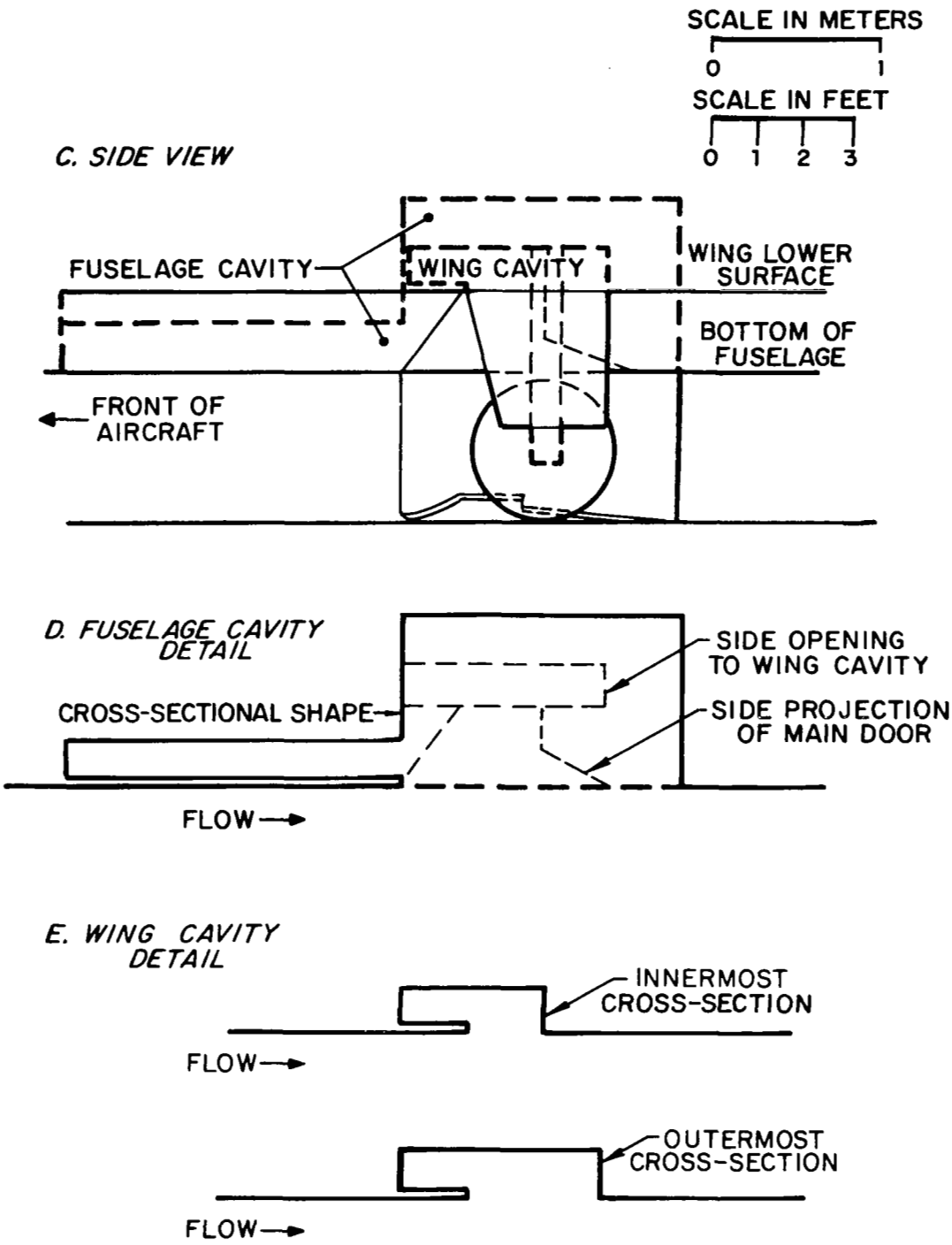

FIG. 6. MCDONNELL-DOUGLAS DC-9 MAIN LANDING GEAR (Concluded).

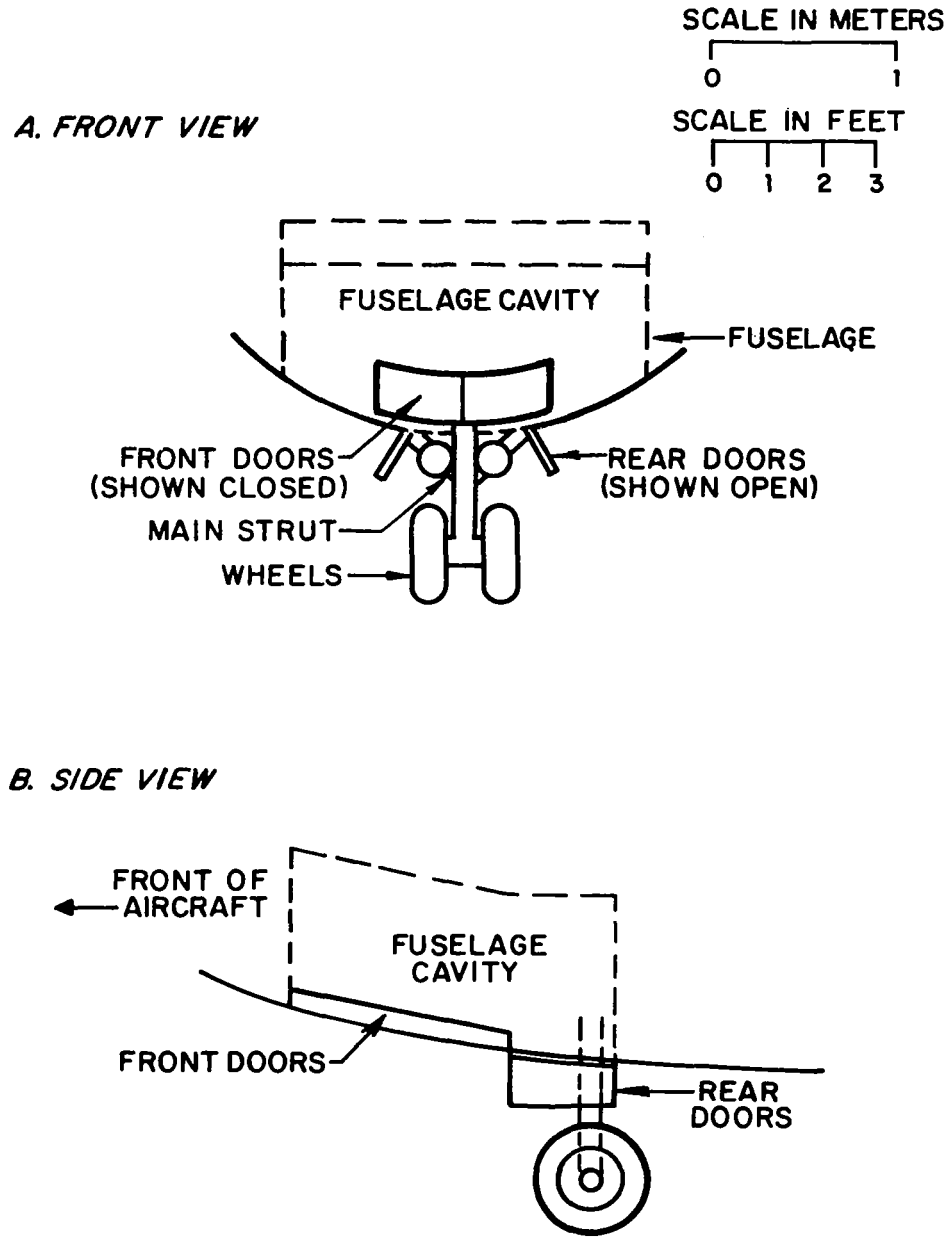

FIG. 7. MCDONNELL-DOUGLAS DC-9 NOSE LANDING GEAR.

Both aircraft have a two-wheel nose gear supported by a single strut. When the gear is lowered two sets of doors open. The larger forward doors reclose once the gear is in place. During the lowering process, the large rectangular cavity which houses the nose gear is open and exposed to the flow. However, the flow over this cavity is seriously disturbed during part of this time by the landing gear itself. Once the gear is in place, the rear doors remain open, producing a relatively small opening into a large internal enclosure. The flow over this opening is seriously disturbed by the presence of the strut which is typically very cluttered with braces, lights, etc. The small doors on the Boeing 727 are also fitted with large curved flow deflectors, whose purpose appears to be to force air into the cavity.

On each side, the main landing gear of both aircraft has a single main strut to support two wheels. There is a diagonal brace running from the main strut, just above the wheels, to the fuselage interior. In their retracted position, the wheels are contained in the fuselage, and the main strut and its pivot point are located in the wing. Thus, there is a small wing cavity and a relatively large fuselage cavity. The door for the wing cavity is open and exposed to the flow whenever the gear is in place. On the Boeing 727, this door also covers a small portion of the fuselage cavity. The fuselage cavity door opens when the gear is being lowered and then recloses once the gear is in place. While it is open, the large essentially rectangular fuselage cavity is exposed to the flow. For part of this time, as the gear leaves the cavity, the flow over the fuselage cavity will be seriously interrupted. The entire process of lowering the main gear and reclosing the fuselage doors takes about 10 seconds. Once the gear is in place, the large fuselage cavity is vented to the external flow only through the wing cavity and, perhaps, a small opening on the adjacent fuselage surface. The wing cavity is bounded in the spanwise direction by the main strut (which extends into its volume) at one end and the opening into the fuselage cavity enclosure at the other end. Except for the main strut and brace, flow over the wing cavity span is relatively unimpaired. The state of the upstream boundary layer is somewhat uncertain since the wing leading edge devices are usually deployed when this cavity is open. The relative locations are such that the inboard termination of the leading edge device may be directly upstream of the wing cavity, suggesting that a vortex may pass over the cavity mouth.

NOISE SOURCE IDENTIFICATION

In this section, the sources of landing gear/cavity noise are identified. In the following sections, these noise sources are discussed in greater detail to show quantitatively their dependence on geometry and flow parameters and to show qualitatively their expected directivity patterns. Sample calculations will be carried out for the Boeing 727 aircraft. The noise sources classified below are essentially due to four mechanisms: modal pressure oscillation phenomena, the edge noise mechanism, vortex shedding, and the impingement of turbulent flow on surfaces and bodies.

Cavity Discrete Pressure Oscillations

Flow over open cavities or cut-outs in the surfaces of aircraft often produces intense pressure oscillations in the cavity which radiates discrete noise. The nature of the cavity response depends on the complex interaction of the cavity internal wave structure and the external shear layer. The mean flow supplies the energy to sustain the oscillation process. As indicated in the previous section, landing gear cavities may be either almost entirely open to the flow on one face or closed except for a small opening to the flow, or to another cavity. The occurrence of oscillations depends on the cavity configuration, the flow speed and upstream boundary layer, and the presence of struts, etc., which may disturb the flow. The cavity oscillation process seems to cause monopole radiation, at least at low speeds.

Cavity Leading Edge Noise

As the turbulent boundary layer flow passes over the cavity leading edges, it experiences a sudden change in surface impedance and substantial sound is radiated. This source behaves as a spanwise array of incoherent acoustic dipoles, whose directivity is modified by the baffling effect of the edge.

Cavity Trailing Edge Noise

Whether or not the cavity oscillates, the cavity trailing edge is subjected to an unsteady inflow due to its interaction with the turbulent shear layer over the cavity mouth. The resulting fluctuating forces will again produce dipole-like acoustic radiation. This noise source will be affected by the presence of struts or protuberances in the cavity shear layer.

Landing Gear Direct Radiated Noise

The struts, wheels, braces, and doors of the landing gear will radiate noise directly due to the fluctuating lift and drag forces produced by vortex shedding from these essentially bluff bodies. The characteristics of the shedding may be affected by the mutual interaction between bodies and by the presence of the cavity shear layer.

Cavity and Gear Wake Interactions with the Wing Trailing Edge and Flaps

The turbulent wakes behind the landing gear cavities and struts may induce unsteady loads on the wing trailing edge and the flap system. These loads are produced by direct turbulence impingement and by the effect of turbulent flow over edges. The resulting impingement noise and edge noise will depend on the turbulence spectrum of the wakes and on the interaction geometry.

Landing Gear Wake/Landing Gear Interactions

On some landing gear configurations, the wakes of some gear components may impinge on other gear components and produce unsteady loads. This type of interaction can be expected on the in-line main struts and wheels of some large aircraft. The importance of this noise source will strongly depend on the particular landing gear geometry.

CAVITY DISCRETE PRESSURE OSCILLATIONS

High speed flow over cavities or cut-outs in the structural surfaces of aircraft often produces intense tonal pressure fluctuations. A basic rectangular cavity configuration is shown in Fig. 8. A typical pressure spectrum measured in such a cavity is shown in Fig. 9, where three discrete peaks can be seen. Substantial research has already gone into the study of cavity oscillations, but most of the work has concentrated on high subsonic and supersonic Mach numbers. As a result, less detailed information is available for the low Mach number subsonic flow case (e.g. $M < 0.3$) of interest in connection with airframe noise, although the underlying oscillation mechanism should be essentially the same. A majority of the work has focused on simple rectangular geometry, which is sometimes, but not always, an

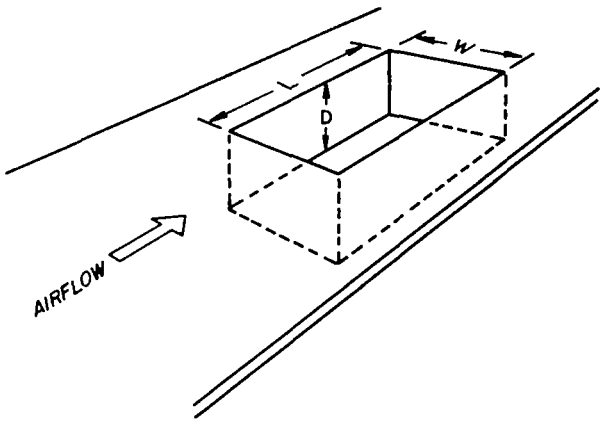

FIG. 8. SIMPLE RECTANGULAR CAVITY.

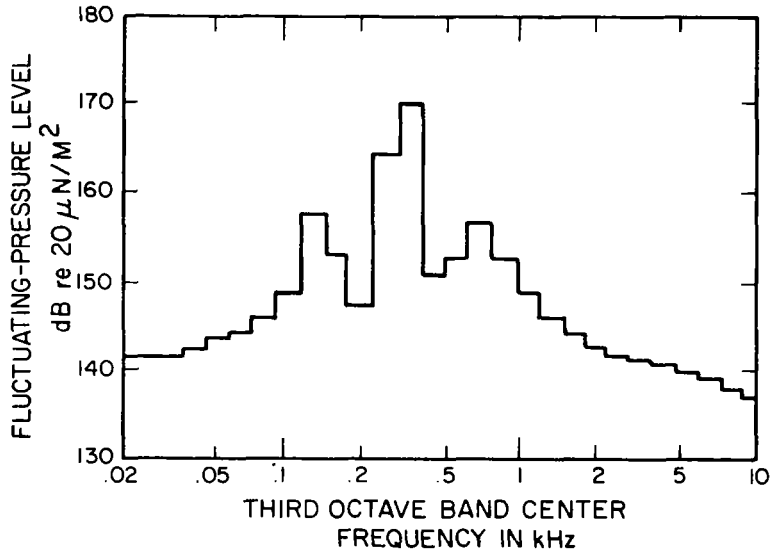

FIG. 9. TYPICAL PRESSURE SPECTRUM MEASURED IN A RECTANGULAR CAVITY.

appropriate representation of landing gear cavity geometry. The recent work of Heller and Bliss (1974 and 1975) provides the basis for much of the following discussion.

In general, cavities oscillate due to a coupling between internal pressure modes and the motion of the shear layer over the cavity mouth. Shear layer deflections at the cavity mouth trailing edge produce mass addition and removal at this point in the cavity. This periodic mass addition and removal forces the acoustic modes in the cavity, which force the shear layer and thereby provide the required shear layer deflection at the trailing edge. Actually, the internal modes and the shear layer motion are coupled and cannot be considered separately. Formally, the shear layer must be treated as a boundary of the system subject to the appropriate material surface and pressure boundary conditions, which couple the internal wave motion to the corresponding wave pattern in the external flow. The importance of properly treating the shear layer coupling is illustrated by the fact that measured modal frequencies in open rectangular cavities differ substantially from the corresponding hard box modes. If the mouth area is a small fraction of the total cavity surface area, then, of course, the effect of shear layer coupling becomes less important, and it may be possible to estimate the frequencies by simpler means. Shallow rectangular cavities, $L/D > 2.0$, tend to respond primarily in lengthwise modes, whereas deep cavities, $L/D < 2.0$, tend to respond in depth modes. For other cavity configurations, the internal modes may be quite complex, but the oscillation mechanism just described still applies.

The shedding of discrete vortices from the cavity leading edge, and their subsequent impingement on the trailing edge, has sometimes been considered essential to the cavity oscillation process. Discrete vortices have often been observed experimentally in the subsonic flow case. Very likely, the rolling up of the shear layer into vortices is a manifestation of the forcing due to the cavity internal pressure modes. In fact, this nonlinear behavior may provide an important amplitude limiting mechanism for the oscillation process.

Since simple rectangular cavities will be used as the basis for some of the noise predictions in this report, it is worthwhile to review the oscillation process for this case in some detail. As mentioned, shear layer deflection leads to a periodic mass addition and removal at the cavity trailing edge. In a shallow cavity, this mass addition and removal produces an effect that is similar to replacing the cavity rear bulkhead with an oscillating piston. (For deeper cavities, a monopole source at the trailing edge would be more appropriate than a piston.)

This "pseudopiston" effect generates forward traveling waves in the cavity that reflect from the front bulkhead to become rearward traveling waves. The resulting wave structure in the cavity forces the shear layer in an unsteady manner over the entire cavity length. This shear layer motion, in turn, is responsible for the trailing edge mass addition and removal that originally produced the cavity internal wave structure; thus, the feedback loop is complete.

Figure 10 shows a typical oscillation cycle as derived from water table flow visualization techniques.* In (A) an upstream traveling wave reaches the front bulkhead while a downstream wave approaches the rear bulkhead. The reflected wave proceeds rearward in (B) and (C), while a new upstream wave is formed at the rear as the shear layer deflects below the trailing cavity edge. The waves interact near the cavity center as shown in (D) and (E). In (F), the waves again approach the front and rear bulkheads, and the shear layer is above the trailing edge level as mass is effectively removed from the cavity. Notice in this illustration that the upstream traveling wave radiates into the external flow whereas the downstream wave does not. This occurs because the upstream wave produces a disturbance which moves supersonically relative to the external flow, while the relative velocity of the downstream wave is subsonic. The phase speeds of the upstream and downstream waves may be considerably different from the sound speed in the cavity because of the effective compliance of the shear layer. Furthermore, the phase speeds are also different from each other because the shear layer appears stiffer to the upstream wave than it does to the downstream wave; the speed of the upstream wave is therefore greater. Similarly, the spatial envelopes of the upstream and downstream waves are different. Typically, the upstream wave radiates and decays and the downstream wave draws energy from the external flow and amplifies. If the energy addition of the downstream wave exceeds the energy loss of the upstream wave by an amount sufficient to overcome all other sources of energy loss in the system, then the oscillation process will sustain itself. The actual amplitude of oscillation is controlled by the level of damping in the system and by the effect of nonlinearity, which ultimately limits the rate of energy removal from the external flow. It is precisely the behavior of the cavity as a very complex oscillator whose amplitude is controlled by many factors that makes even the semi-empirical prediction of oscillation amplitudes difficult.

The combination of the upstream and downstream waves in the cavity produces a standing wave pattern whose peak pressure amplitudes increase toward the trailing edge. Typical experimental mode shapes are shown in Fig. 11. A pressure amplitude

*Although strictly speaking, the water table simulation applies to Mach number flows, the processes illustrated are believed to be essentially the same for low Mach number flow.

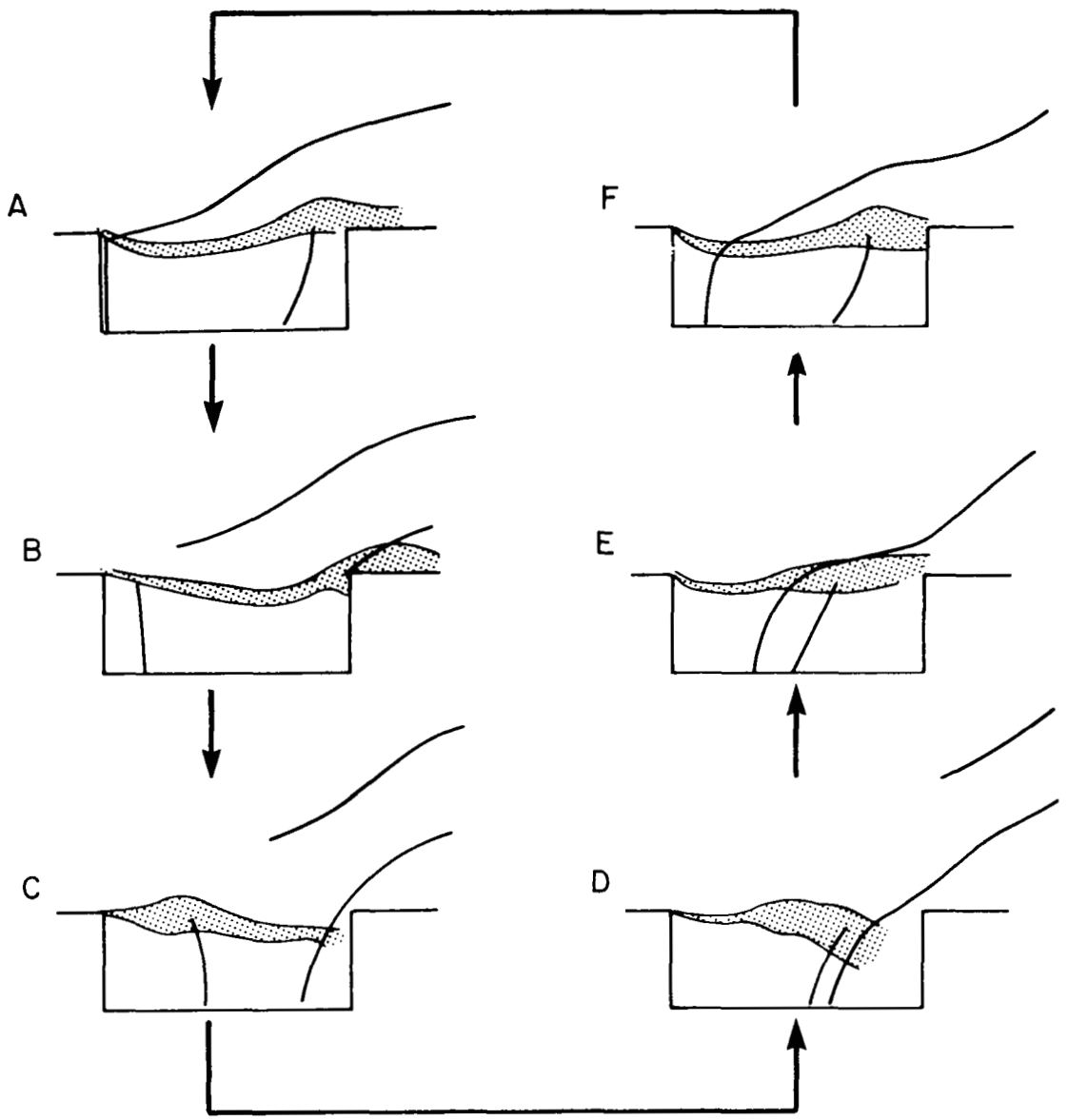

FIG. 10. TYPICAL OSCILLATION CYCLE.

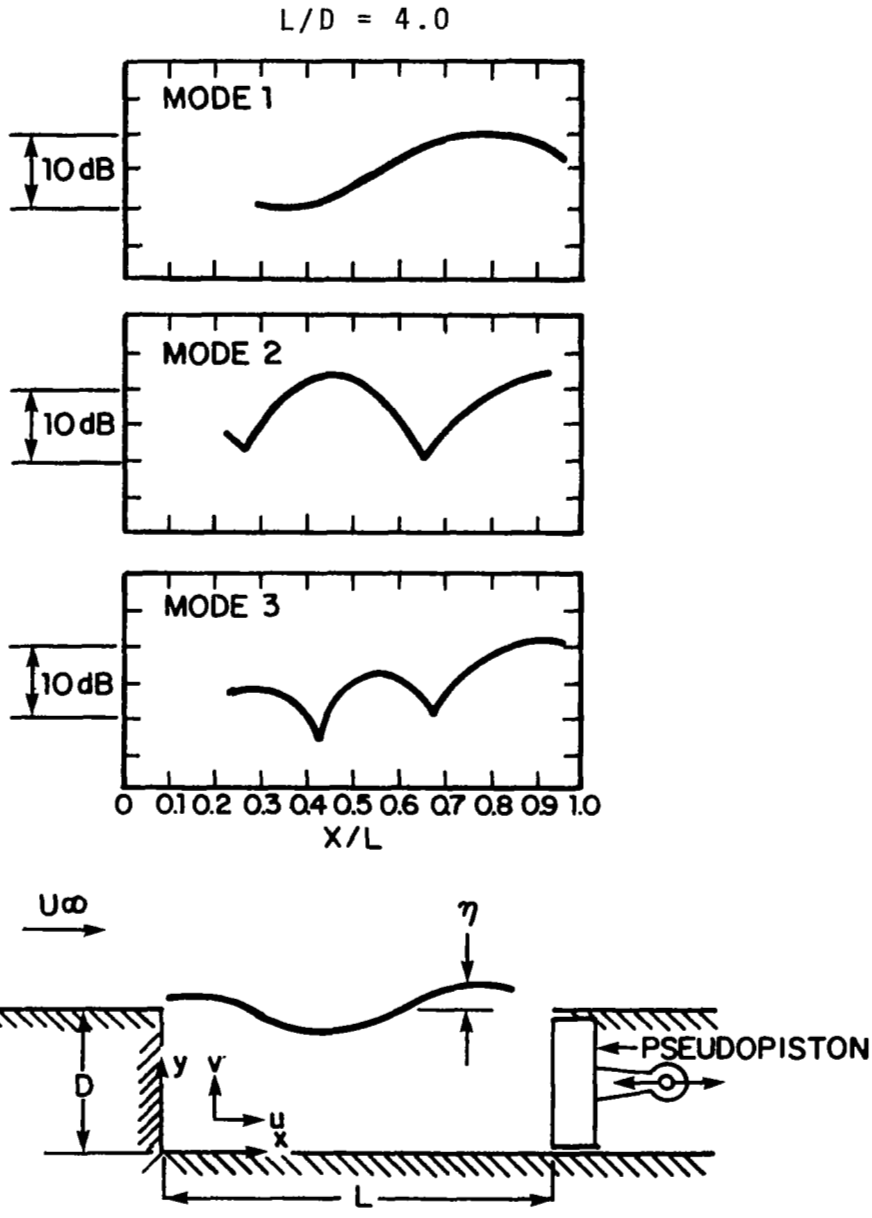

FIG. 11. TYPICAL EXPERIMENTAL MODE SHAPES AND THE PSEUDOPISTON ANALOGY (DATA FOR M = 0.8).

maximum always occurs at the front bulkhead, but often the corresponding maximum at the rear does not occur exactly at the wall. This displacement of the rearward maximum is a manifestation of the piston-like effect of periodic mass addition and removal at the trailing edge.

If the oscillation frequencies are re-expressed as a Strouhal number based on free stream speed and cavity length, and then plotted against Mach number, they order themselves along certain lines that can be associated with resonant modes as shown in Fig. 12. The solid lines correspond to the semi-empirical equation

$$S_m = \frac{f_m L}{U_\infty} = \frac{m-\alpha}{\left[M/\sqrt{1+\frac{\gamma-1}{2}M^2}\right] + 1/k_v} \qquad (1)$$

where m is the mode number (equal to 1, 2, 3,...), $\gamma = 1.4$ is the ratio of specific heats. The quantities α and k_v are empirical constants; the choice of $\alpha = 0.25$ and $k_v = 0.57$ is in good agreement with the experimental data. A semi-empirical frequency formula similar to the above was first given by Rossiter (1966). The present form, presented by Heller *et al.* (1970), corrects for the higher sound speed in the cavity, which nearly equals the free-stream stagnation sound speed. Unfortunately, Eq. (1) agrees least well with the data at low Mach number. Furthermore, the data begins to show some length-to-depth ratio, L/D, dependence at low Mach number as evidenced by the systematic spreading for each mode number. This dependence is not accounted for by Eq. (1). Nevertheless, Eq. (1) will provide a satisfactory rough estimate of frequency in the low Mach number range as long as the cavity remains shallow. It can, however, be seriously in error for deep cavities.

Figures 13 and 14 illustrate cavity pressure levels at the front and rear bulkheads, respectively, as a function of mode number, length-to-depth ratio, and Mach number. Different modes are seen to dominate depending on the particular conditions. For the cases where there is adequate data, the levels are seen to drop very dramatically at low Mach number. Experiments show that there is usually a Mach number below which a given cavity will not exhibit discrete oscillations, i.e., an initial onset speed. Aircraft landing gear cavities may well fall in the vicinity of initial onset. The data does clearly illustrate that no simple relation between level and speed is evident. Again, this complication arises because the cavity behaves as an oscillator whose amplitude is controlled by complex processes.

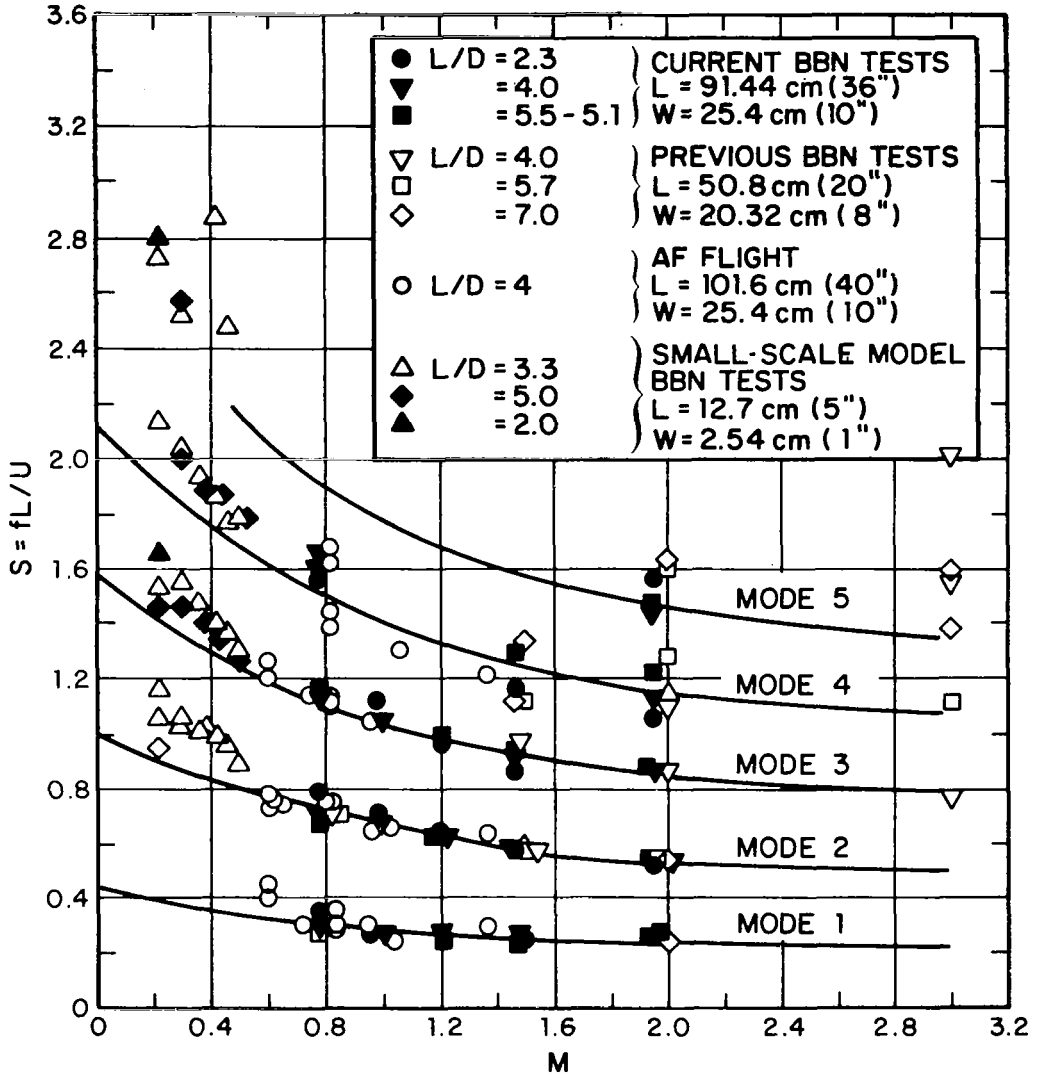

FIG. 12. STROUHAL FREQUENCIES OF CAVITY MODES AS A FUNCTION OF MACH NUMBER.

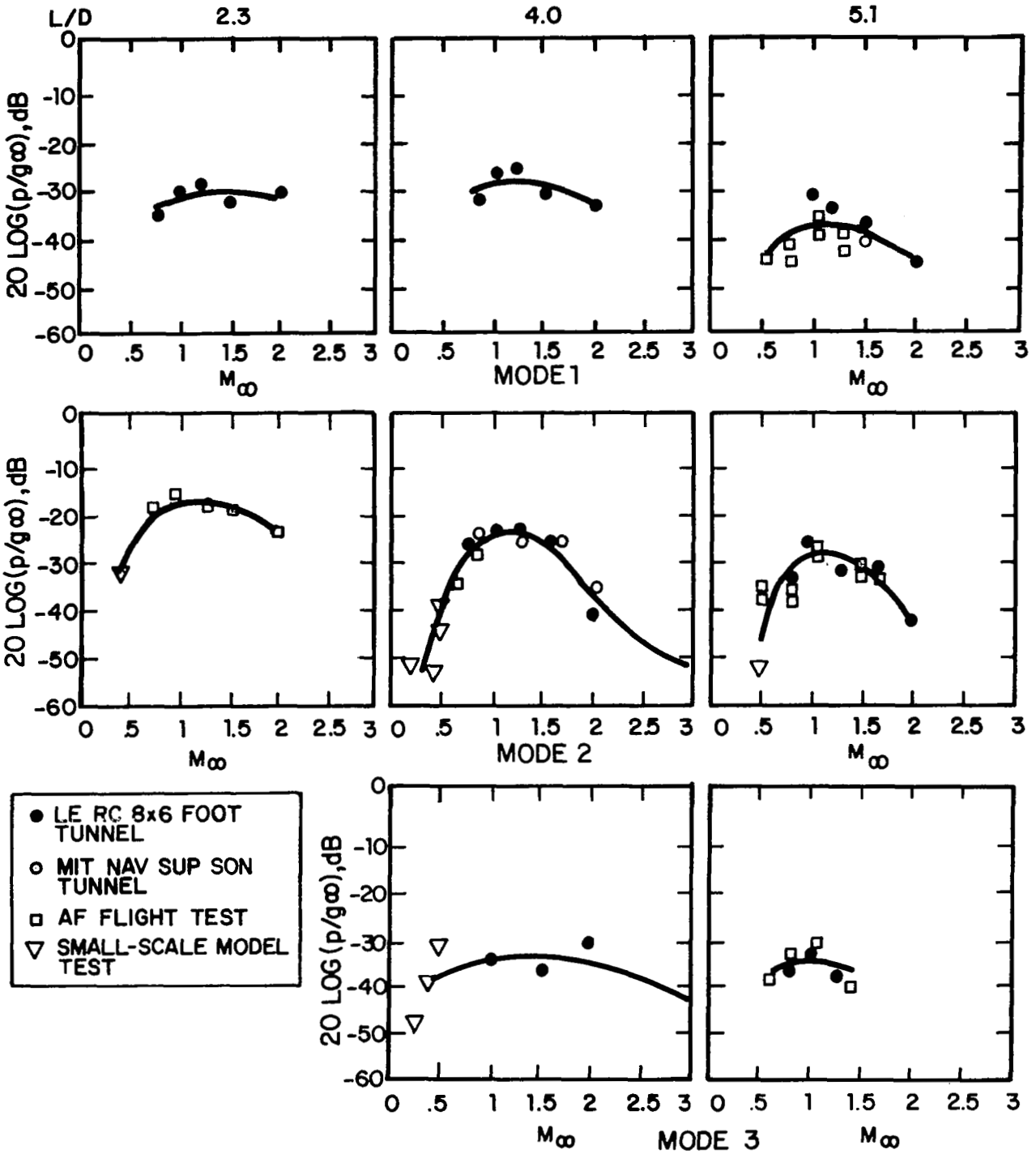

FIG. 13. COMPARISON OF MACH NUMBER DEPENDENCIES OF RESONANT MODE LEVELS: LEADING-EDGE AREA.

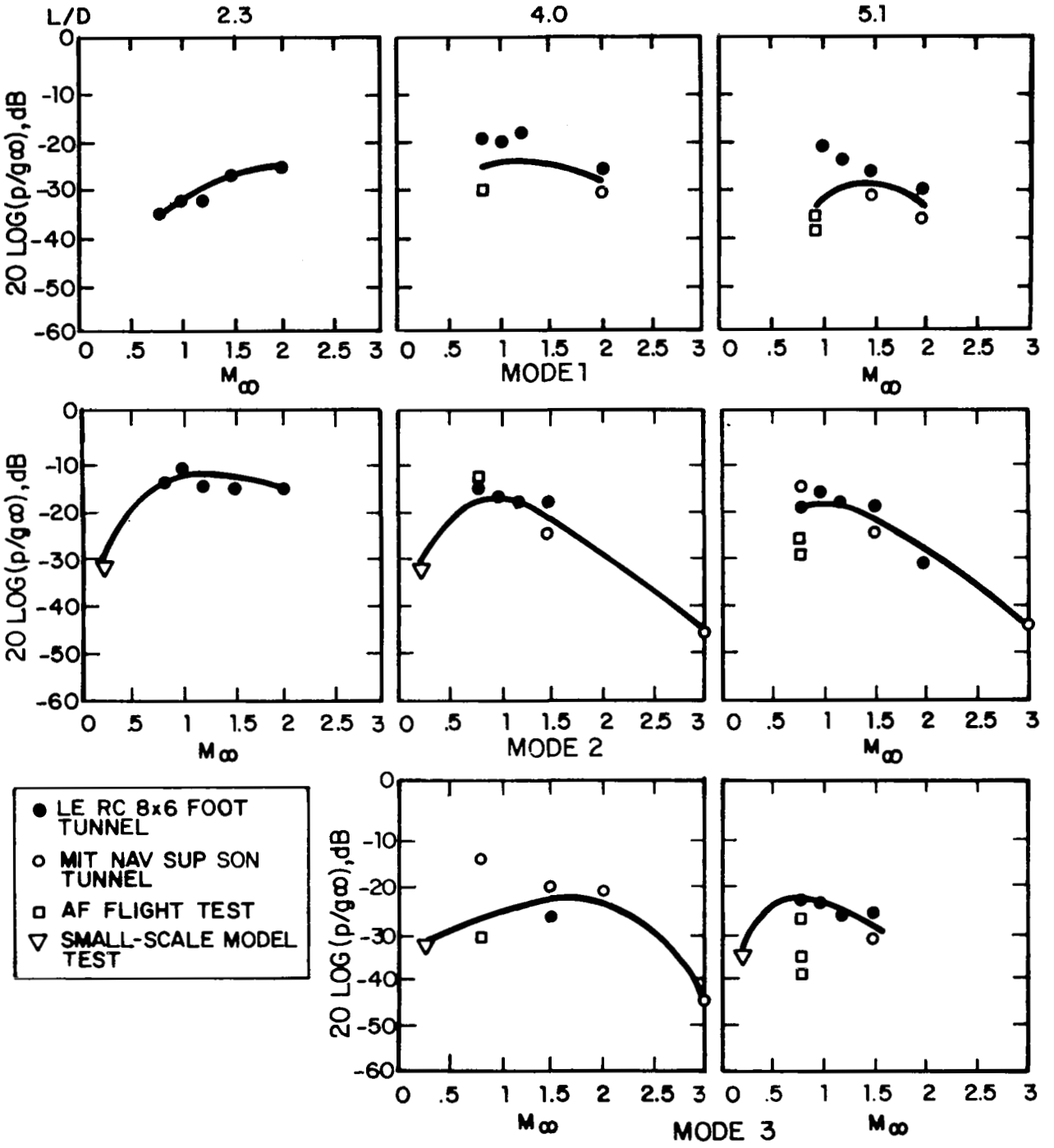

FIG. 14. COMPARISON OF MACH NUMBER DEPENDENCIES OF RESONANT MODE LEVELS: TRAILING-EDGE AREA.

The external radiation pattern for high speed subsonic flow is shown in Fig. 15. This sketch is consistent with both the oscillation process described previously and the flow visualization photographs available in the literature. Directivity measurements taken on a small scale cavity model in a wall jet facility suggest that at very low Mach numbers the radiation pattern is not as directional as indicated and is, for all practical purposes, that of a simple monopole (Heller, 1974). It can be concluded that the directional structure indicated in Fig. 15 becomes less pronounced with decreasing Mach number. This trend is supported by the photographs of Karamacheti (1955). The strength of the monopole radiation will be directly related to the trailing edge mass addition and removal process.

Assuming a cavity radiates as a simple monopole,*

$$\overline{p^2} = \frac{\rho^2}{4r^2} f^2 \overline{Q^2} \quad , \tag{2}$$

where r is the distance from the source and Q is the amplitude of the unsteady mass flow. Because Q must be directly related to the unsteady mass addition and removal process at the cavity trailing edge, we can write

$$\sqrt{\overline{Q^2}} = \frac{1}{\sqrt{2}} \frac{U_\infty}{2} W\eta\beta \quad , \tag{3}$$

where $U_\infty/2$ is the average velocity in the shear layer, W is the cavity width, η is the shear layer perturbation amplitude at the trailing edge, and β is a correction factor discussed below. The shear layer amplitude can be nondimensionalized by the cavity length:

$$\eta = \hat{\eta} L \quad . \tag{4}$$

Then,

$$\overline{p^2} = \left[\frac{1}{2\sqrt{2}} \left(\frac{1}{2} \rho U_\infty^2\right) \left(\frac{fL}{U_\infty}\right) \left(\frac{W}{r}\right) \hat{\eta}\beta \right]^2 = \left[\frac{\beta\hat{\eta}}{2\sqrt{2}} qS \frac{W}{r} \right]^2 , \tag{5}$$

where q is the dynamic pressure and S is the Strouhal number, given approximately by Eq. (1) as a function of mode number and Mach number. The corresponding total power is given by

*Due to the fairly low frequencies with correspondingly long wavelengths, and the actual locations of cavities on the aircraft, we have chosen to neglect any effect of the aircraft as an acoustic baffle.

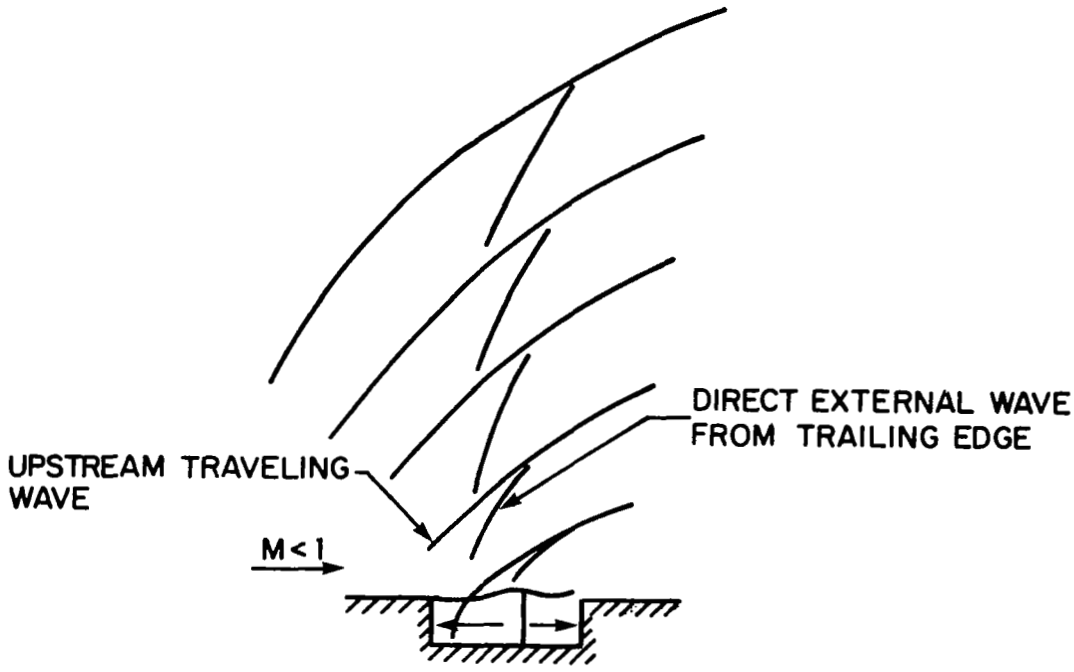

FIG. 15. TYPICAL CAVITY EXTERNAL RADIATION PATTERN IN HIGH SPEED SUBSONIC FLOW (M_∞>0.5).

$$\Pi = \frac{\pi}{2\rho c} \left[\beta \hat{\eta} q S W\right]^2 \quad . \tag{6}$$

The nondimensional shear layer amplitude, $\hat{\eta}$, may depend on a number of parameters, but primarily

$$\hat{\eta} = \hat{\eta} \left(M, \frac{L}{D}, \frac{fD}{a_c}, \frac{\delta}{L}\right) \quad .$$

The dependence on fD/a_c contains information on the ratio of wavelength to depth. Dependence on M, L/D, and fD/a_c is indicated by the analytical work of Heller and Bliss (1974). The ratio of upstream boundary layer thickness to cavity length, δ/L, is an important parameter for the shear layer thickness. The other nondimensional term in Eq. (5) is the flow rate correction factor, β. This factor accounts for the nonuniform shear layer velocity profile, amplitude variations across the cavity width, and other effects associated specifically with the fluid mechanical details of the mass addition and removal process. The most important functional dependences are expected to be

$$\beta = \beta \left(\hat{\eta}, M, \frac{\delta}{L}, \frac{W}{L}\right) \quad .$$

Notice, in particular, that β may depend on the nondimensional amplitude $\hat{\eta}$. In spite of this complexity, we can expect β to be of order unity, the the other terms in Eq. (3) should constitute a proper order-of-magnitude estimate for Q. It is now apparent that the complicated dependence of $\hat{\eta}$ limits the usefulness of Eq. (5).

A rough estimate of levels can be made assuming the shear layer displacement cannot greatly exceed its half thickness. Then, for a turbulent shear layer, let

$$\hat{\eta} = 0.1$$

and assume that $\beta = 1.0$. Because we are interested in the low Mach number limit, Eq. (1) is approximately

$$S = 0.6 \, (m - 1/4) \quad .$$

Then, Eq. (4.5) becomes

$$\overline{p^2} = \left[\frac{0.1}{2\sqrt{2}}\, q\, \frac{W}{r}\, S\right]^2 = \left[.0212\ (m-\tfrac{1}{4})\ q\ \frac{W}{r}\right]^2 , \qquad (7)$$

which will usually be a high estimate, and which is applicable only for low Mach number. The direct dependence on mode number is a result of the approximations made and must not be taken too seriously. Clearly, it should not be used for high mode numbers (e.g., $m > 4$).

When some experimental data is available, the dependence of $(\hat{\eta}\beta)$ in Eq. (5) can be estimated. The dependences on M and L/D are probably strongest. Therefore,

$$(\hat{\eta}\beta) \approx k_1 M^{k_2} , \qquad (8)$$

where k_1 and k_2 are constants which depend on L/D. The approximation of Eq. (8) is useful when some data is available at two Mach numbers that are not too widely separated. It is then possible to solve for k_1 and k_2 and use Eqs. (8) and (5) to predict the radiation from other cavities assumed similar to these for which data is available. This is the approach used to predict discrete tone noise from landing gear cavities. Substituting Eq. (8) into Eq. (5) gives

$$\overline{p^2} = \left[k_1 M^{k_2}\ \frac{1}{2\sqrt{2}}\ qS\ \frac{W}{r}\right]^2 . \qquad (9)$$

The corresponding total power level is

$$\Pi = \frac{\pi}{2\rho c}\left[k_1 M^{k_2}\ qSW\right]^2 . \qquad (10)$$

The cavity tone frequencies and levels for the Boeing 727 aircraft will not be estimated. Table 1 summarizes data obtained by Heller (1974), which is useful for the estimation procedure. In addition, Figs. 12, 13, and 14 will be used as required. Table 2 summarizes the cavity geometry for the main loading gear fuselage and wing cavities and the nose gear cavity. The aircraft approach speed is assumed to be 73 m/sec (240 ft/sec), with $M = .215$ and $q = 3280\ N/m^2$ ($68.5\ lb/ft^2$). SPL is referred to $20\ \mu N/m^2$ and PWL is referred to 10^{-12} watts. SPL is determined at 152.4 m (500 ft) below and 152.4 m (500 ft) to the side of the aircraft ($r = 152.4 \times \sqrt{2}$ m) assuming monopole directivity.

TABLE 1. SUMMARY OF EXPERIMENTAL DATA (TURBULENT BOUNDARY LAYER)

Run No.	L/D	U_∞ m/sec (ft/sec)	M	q,N/m² (lb/ft²)	f,Hz	$S=fL/U_\infty$*	Level, Mic. No. 1, dB†	Level, Mic. No. 4, dB**	Pred. Eq. (7)‡
10	1.0	42.7 (140)	.125	1116 (23.3)	1200	1.79	98	81	97.2
11	1.4	42.7 (140)	.125	1116 (23.3)	1000	2.08	99	84	98.5
12	1.6	42.7 (140)	.125	1116 (23.3)	1050	2.50	96	81	100.1
13	2.0	85.3 (280)	.251	4462 (93.2)	1150	1.71	109	95	108.8
14	1.6	85.3 (280)	.251	4462 (93.2)	1000	1.19	120	106	105.7
15	1.4	85.3 (280)	.251	4462 (93.2)	1000	1.04	126	108	104.5
16	1.0	85.3 (280)	.251	4462 (93.2)	1250	0.93	106	90	103.5
17	4.0	85.3 (280)	.251	4462 (93.2)	2000	2.98	106	88	111.4

Note: W = 2.54 cm for all cases. D = 6.35 cm except for Run No. 17 where D = 3.18 cm.

*Dominant mode.

†Microphone 1 was located in the cavity front bulkhead.

**Microphone 4 was located 86.4 cm directly above the cavity mouth.

‡Using measured S.

TABLE 2. CAVITY GEOMETRY FOR THE BOEING 727 AIRCRAFT

	L,m (ft)	D,m (ft)	W,m (ft)	L/D	Volume m^3 (ft^3)	Mouth Area m^2 (ft^2)
Main Gear Fuselage Cavity						
Fuselage door open	2.04 (6.7)	1.68 (5.5)	1.74 (5.7)	1.2	5.95 (210.0)	3.55 (38.2)
Fuselage door closed	1.28 (4.2)	1.74 (5.7)	1.13 (3.7)	-	5.95 (210.0)	1.46 (15.7)*
Main Gear Wing Cavity						
Innermost	1.43 (4.7)	0.61 (2.0)	-	2.3	-	-
Outermost	0.88 (2.9)	0.61 (2.0)	-	1.5	-	-
Average	1.16 (3.8)	0.61 (2.0)	1.01 (3.3)†	1.9	0.89 (31.3)	1.16 (12.5)
Nose Gear Cavity						
All doors open	2.68 (8.8)	0.85 (2.8)	1.07 (3.5)	3.2	2.41 (85.0)	2.86 (30.8)
Main doors closed	1.31 (4.3)	0.85 (2.8)	1.01 (3.3)	-	2.41 (85.0)	1.32 (14.2)

*Includes opening into wing cavity; values of L and W are averages.

†Excludes portion occupied by main gear strut.

Main Gear Fuselage Cavity

When the doors are open, the main fuselage cavity has an L/D = 1.2. By approximating this as L/D = 1.0, runs 10 and 16 can be used in Eq. (9) to find $k_1 = 0.0388$ and $k_2 = 0.442$. Because this is a deep cavity, the frequency is nearly independent of speed, so the Strouhal number behaves as the inverse speed; interpolating, we find S = 1.05 at $U_\infty = 73.2$ m/sec (240 ft/sec). From Eqs. (10) and (9):

PWL = 137 dB , SPL = 76 dB , f = 38 Hz.

For comparison, Eq. (7) predicts SPL = 94 dB, using S = 1.05.

Main Gear Wing Cavity

The average L/D is 1.9, but we assume 1.6 to use the data of Table 1. Using runs 12 and 14 with Eq. (9) gives $k_1 = 9.1$ and $k_2 = 3.23$. Interpolating the data of Table 1 gives S = 1.65. From Eqs. (10) and (9):

PWL = 138 dB , SPL = 83 dB , f = 104 Hz.

For comparison, Eq. (7) predicts SPL = 93 dB.

Nose Gear Cavity

When all the doors are open, the nose gear cavity has an L/D = 3.2. From the data for L/D = 3.3 in Fig. 12, we have S = 1.05 for Mode 2 and S = 1.5 for Mode 3. Since Table 1 has no external radiation levels for this case it is necessary to improvise. Using Fig. 13 with L/D = 4.0, the level at the cavity leading edge bulkhead is approximately

$$20 \log \frac{P}{q} = -53 \text{ dB for Mode 2}$$

$$20 \log \frac{P}{q} = -47 \text{ dB for Mode 3}$$

Observe from Table 1 that there was about a 15 dB average difference between the levels at microphones 1 and 4. Using the above, the equivalent levels at microphone 4 can be estimated as

96 dB for Mode 2 and 102 dB for Mode 3. Then, using Eq. (5), calculate $\beta\hat{\eta} = 0.038$ for Mode 2, and $\beta\hat{\eta} = 0.118$ for Mode 3. Applying Eqs. (5) and (6) to the actual case gives

Mode 2: PWL = 141 dB , SPL = 77 dB , f = 29 Hz

Mode 3: PWL = 153 dB , SPL = 90 dB , f = 41 Hz.

For comparison, Eq. (7) predicts 77 dB for Mode 2, 81 dB for Mode 3, and 84 dB for Mode 4. Using the data of Table 1 directly (assuming L/D = 4.0) gives an estimate of SPL = 70 dB and f = 81 Hz, which corresponds to Mode 4.

Clearly, the above estimates are very approximate and somewhat arbitrary. Equation (7) can provide a simple first estimate with the understanding that the actual answer may be as much as 20 dB lower. The last column of Table 1 suggests that Eq. (7) is most accurate when the cavity oscillates intensely. Beyond this, the above illustrates that obtaining more accurate estimates is directly related to the availability of relevant experimental data. All the different modes that might occur were not estimated. The experimental evidence suggests that Modes 2, 3, and 4 are most commonly observed at dominant levels in this Mach number range. The first two calculations illustrate the point that care must be taken to estimate the proper Strouhal number when the cavity is no longer shallow, e.g., L/D < 2. As the depth scale becomes important, the Strouhal numbers can begin to differ from those of Fig. 12. Decreasing Mach number seems to accentuate this difference.

The discussion and estimates so far have assumed clean rectangular cavities. In fact, the landing gear cavities on real aircraft are not always simply rectangular and are usually cluttered with struts, braces, and doors. The wing cavities often have a substantial leading edge overhang and nonconstant length. At one end, the wing cavity opens into a large fuselage volume, and at the other end it is disturbed by the main landing gear shaft. The state of the upstream flow may be uncertain because leading edge devices are often deployed when the cavity is open. As mentioned earlier, during part of the short time that the main doors on the fuselage and nose are open, the gear is in the process of being deployed, and the flow over the cavity mouth is seriously interrupted.

All of the above factors can be expected to reduce the level of oscillations and, in some cases, suppress them entirely. Recently, Heller and Bliss (1974) studied a number of possible

oscillation suppression devices. Much of this research concentrated on the high subsonic and supersonic Mach number range, where cavity oscillations are particularly intense. One way found to reduce the oscillation levels was to disturb the upstream flow and cavity shear layer with spoilers or vortex generators. These results suggest that any disturbances to the flow over the cavity mouth may lead to a substantial reduction in oscillation levels. Very little is known about the effect of venting an open rectangular cavity to a large internal volume like the typical wing cavity configuration. At the very least, the modal pattern in the open cavity will be altered and a reduction in oscillations associated directly with the open cavity can be expected. One effect of the front overhang on wing cavities will be to alter the oscillation frequency. Since wave speeds will be higher under the (noncompliant) overhang, a frequency increase is expected. The effect of a front overhang on levels is unknown; experiments have shown that a rear overhang often increases levels.

In summary, the estimates show that open rectangular cavities can be a significant airframe noise source, but only if realistic landing gear cavities actually do oscillate. During approach, once the main doors have reclosed, the large fuselage and nose cavities become essentially vented enclosures, rather than open rectangular cavities. The flow over the openings will be disturbed by the gear struts and braces. The opening of the nose gear cavity is particularly cluttered. There is presently no reliable way to estimate the oscillation levels for these enclosures. However, oscillation frequencies will be approximately given by the Helmholtz resonator frequency and by the hard modes. These frequencies have been estimated for the Boeing 727 and are presented in Table 3. It is not presently known whether these vented enclosures can be a significant source of airframe noise.

CAVITY LEADING EDGE NOISE

When a turbulent boundary layer encounters an abrupt change in surface impedance, such as an edge, substantial sound is radiated. This situation occurs when the turbulent boundary layer passes over the landing gear cavity leading edges. The process can be modeled as a spanwise array of incoherent dipoles whose force strength is related to the fluctuating pressure at the surface and the correlation area of the local disturbance. The directivity of these edge sources differs from the classical dipole by virtue of the presence of a baffling surface whose dimensions are many characteristic wavelengths of the edge-generated sound. The intensity of this simple modified dipole

TABLE 3. VENTED ENCLOSURE FREQUENCIES FOR BOEING 727 LANDING GEAR CAVITIES

Cavity	Mode	Frequency (Hz)
Main Gear Fuselage Cavity (fuselage doors closed)	Helmholtz Resonator	30
	First Length Mode	84
	First Depth and Width Mode	102
Nose Gear Cavity (forward doors closed)	Helmholtz Resonator	41
	First Length Mode	63
	First Depth Mode	202
	First Width Mode	160

Note 1: Helmholtz resonator frequency: $f = \frac{a_c}{2\pi}\sqrt{\frac{A^2}{(Al)V}}$

where a_c is the cavity sound speed, V is the cavity volume, A is the mouth area (see Table 2) and (Al) is the volume at the resonator mouth.

$(Al) \approx 1.27\ m^3$ $(45\ ft^3)$ main gear cavity

$(Al) \approx 1.33\ m^3$ $(47\ ft^3)$ nose gear cavity.

Note 2: General volume mode frequencies are given by

$$f = \frac{a_c}{2}\sqrt{\left(\frac{n_x}{\ell_x}\right)^2 + \left(\frac{n_y}{\ell_y}\right)^2 + \left(\frac{n_z}{\ell_z}\right)^2}$$

where ℓ_x, ℓ_y, and ℓ_z are the length, depth, and width dimensions, and the integers n_x, n_y, n_z ($n_1 = 0, 1, 2, \ldots$) are corresponding mode numbers.

model is given by

$$I(r,\theta,\psi,\omega) = m \frac{\omega^2 \overline{F^2}}{12\pi\rho c^3 r^2} \sin^2\theta \cos^2\psi/2 \quad , \qquad (11)$$

where ω is the frequency of the fluctuating force, $\overline{F^2}$ is the local mean-square force, m is the effective number of source regions along the span, θ is the angle between the line of the trailing edge and the observer, and ψ is the angle between the plane of the surface and the observer. The number of source regions can be approximated by the span of the edge divided by the spanwise correlation distance in the boundary layer.

Sufficiently detailed measurements of near-edge flows have not been made to allow a direct calculation of radiated sound from the surface pressure spectrum. However, one can take advantage of empirical procedures to estimate edge noise spectra [see Hayden (1972), Hayden *et al.* (1974), and Hayden *et al.* (1975)]. Based on these sources, the spectrum for a lightly loaded airfoil shown in Fig. 16 and the corresponding equation given below were used to estimate cavity loading edge noise for the Boeing 727 aircraft. The equation for overall power level is

$$PWL \text{ (dB re } 10^{-12}\text{w)} = +16.3 + 10 \log (\delta W U^6) \quad . \qquad (12)$$

where δ is the boundary layer thickness (m), W is the cavity width normal to the flow (m), and U is the free stream velocity (m/sec). This expression is valid for the contribution of the flow on one side of the edge, as is appropriate for the cavity leading edge problem.

The computed result for the sum of all possible cavity leading edges exposed to the flow is shown later in Fig. 16. A cavity leading edge boundary layer thickness of 0.055 m (1.18 ft) was used, based on a flat-plate turbulent boundary layer formula and the average distance to the wing leading edge. Actually, the boundary layer properties may be considerably different, since the main gear cavity is located at the wing-fuselage junction and is partially downstream of the wing leading edge devices. However, a more reliable estimate of the boundary layer properties is not available. The same thickness was assumed for the nose gear cavity. No attempt was made to compute separately the case of main fuselage doors and forward nose doors closed, for which the levels will be lower. Because this is a relatively weak noise source, only an upper bound estimate is needed. Note that the length of exposed edge is much less than the length of wing, flap, and stabilizer trailing edges that generate noise by the same mechanism.

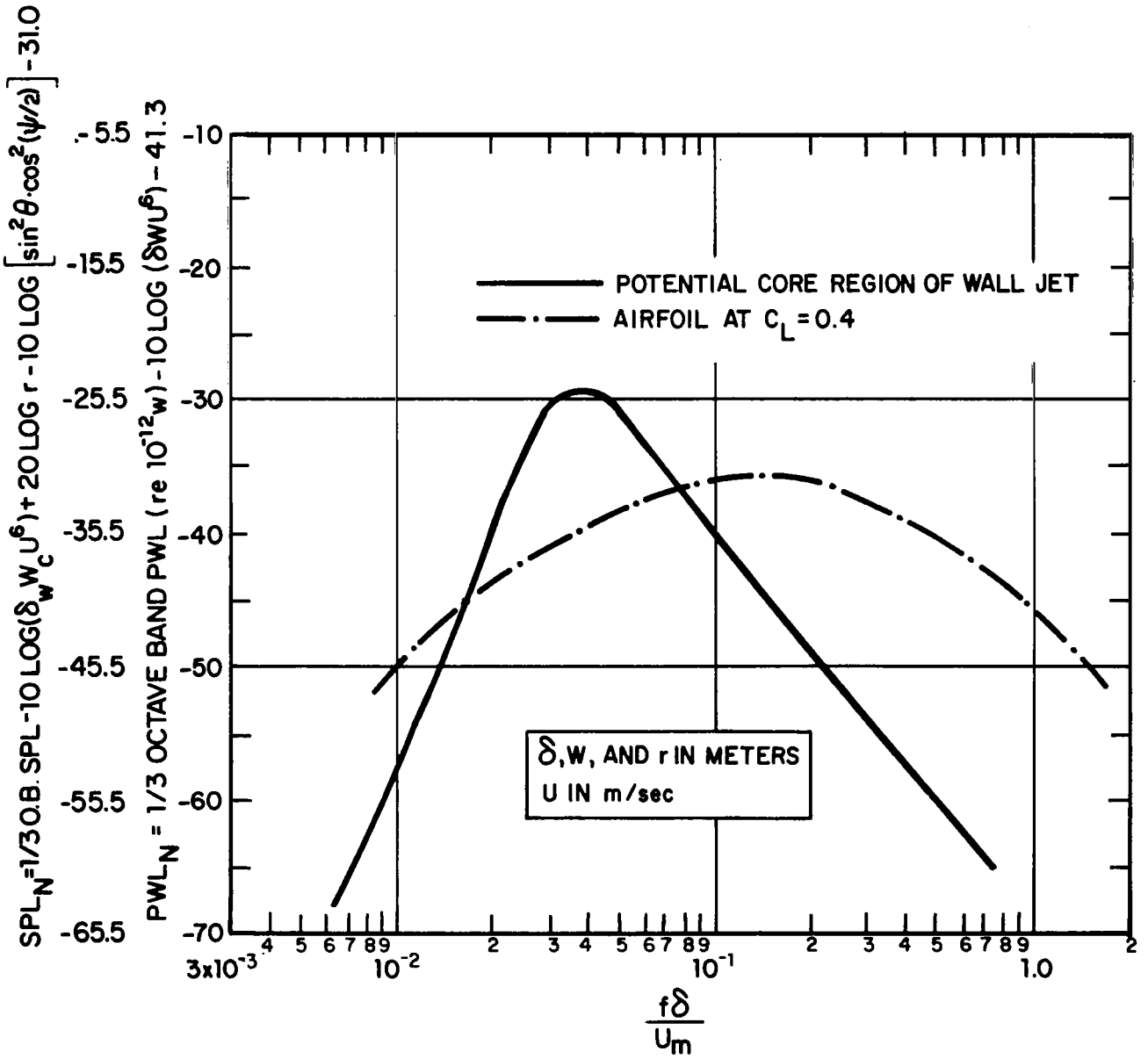

FIG. 16. NONDIMENSIONAL SPECTRUM FOR THE CALCULATION OF CAVITY LEADING EDGE NOISE.

CAVITY TRAILING EDGE NOISE

Regardless of whether or not a cavity oscillates, the cavity trailing edge is subjected to a turbulent inflow due to the presence of the turbulent shear layer over the cavity mouth. The resulting fluctuating forces produce dipole-like acoustic radiation, and are, no doubt, a major source of cavity broadband noise. Figure 17a schematically illustrates this impingement of turbulent inflow, and also gives an indication of the leading edge source discussed in the previous section. Figure 17b indicates qualitatively the anticipated directivity patterns for these sources, which, presumably, are distorted by the presence of the cavity.

The sound mechanism is essentially the leading edge dipole, whose intensity has the same parameter dependences as indicated by Eq. (11). Because of the complexity of the interaction process, it is necessary, however, to employ an empirical scheme. The dipole edge noise model was adapted to the leading-edge situation, and a series of experiments performed using a free jet as a representative source of a free turbulent shear layer. The rationale for the modeling was the same as in other edge noise models; namely, that each local force fluctuation is related to the differential pressure across the edge and the scale of the disturbance. To predict the total sound output, one simply adds up the individual sources, whose numbers are estimated by the ratio of the wetted span, W, to the spanwise correlation length. Figure 18 summarizes the result of several experiments performed by Hayden, Kadman, and Chanaud (1972). The peak power level occurs at a Strouhal number of about 0.3 based on the local shear layer thickness, δ, and the maximum mean velocity, U.

The 1/3-octave band power level at this peak is

$$\text{PWL } (@\ f\delta/U \approx 0.3) \text{ in dB re } 10^{-12}\,\text{w}$$

$$= +8.3 + 10 \log (\delta W U^6) \quad , \tag{13}$$

where δ is the local shear layer thickness in meters ($\delta \approx 0.2x$, where x is the distance from the flow separation point), W is the wetted span (m), and U is the free stream velocity (m/sec). The one-third octave spectrum may be calculated using Fig. 18. Figure 18 also shows variations encountered from positioning effects of the edge in the shear layer and the impingement angle. The

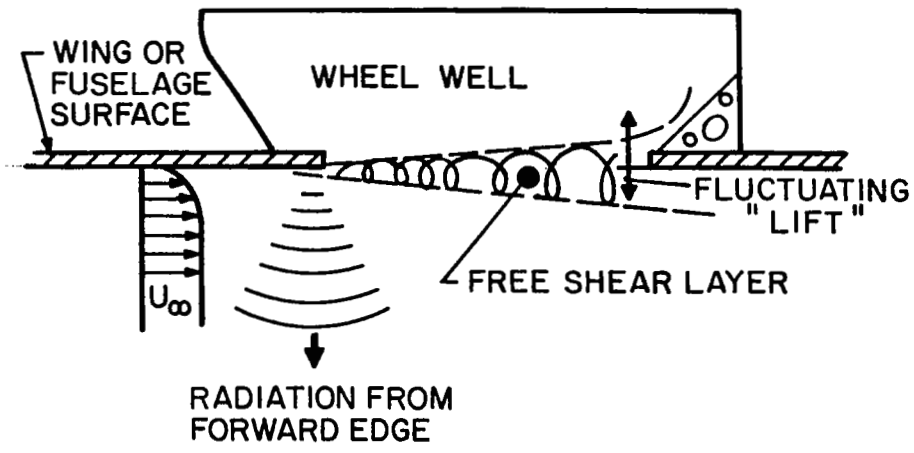

(a) FLOW FIELD ENVIRONMENT

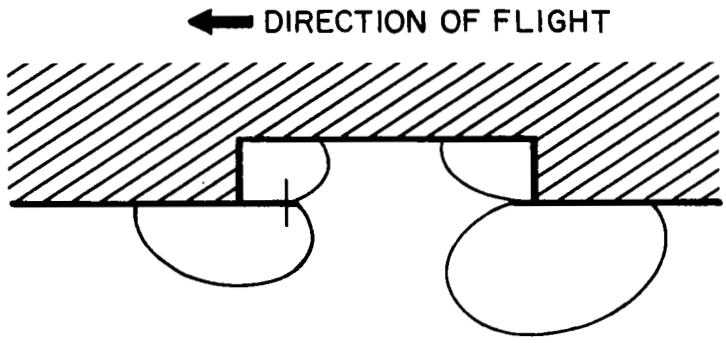

(b) APPROXIMATE RADIATION PATTERNS FROM EDGE SOURCES

FIG. 17. CAVITY EDGE NOISE MECHANISMS AND THEIR APPROXIMATE DIRECTIVITY.

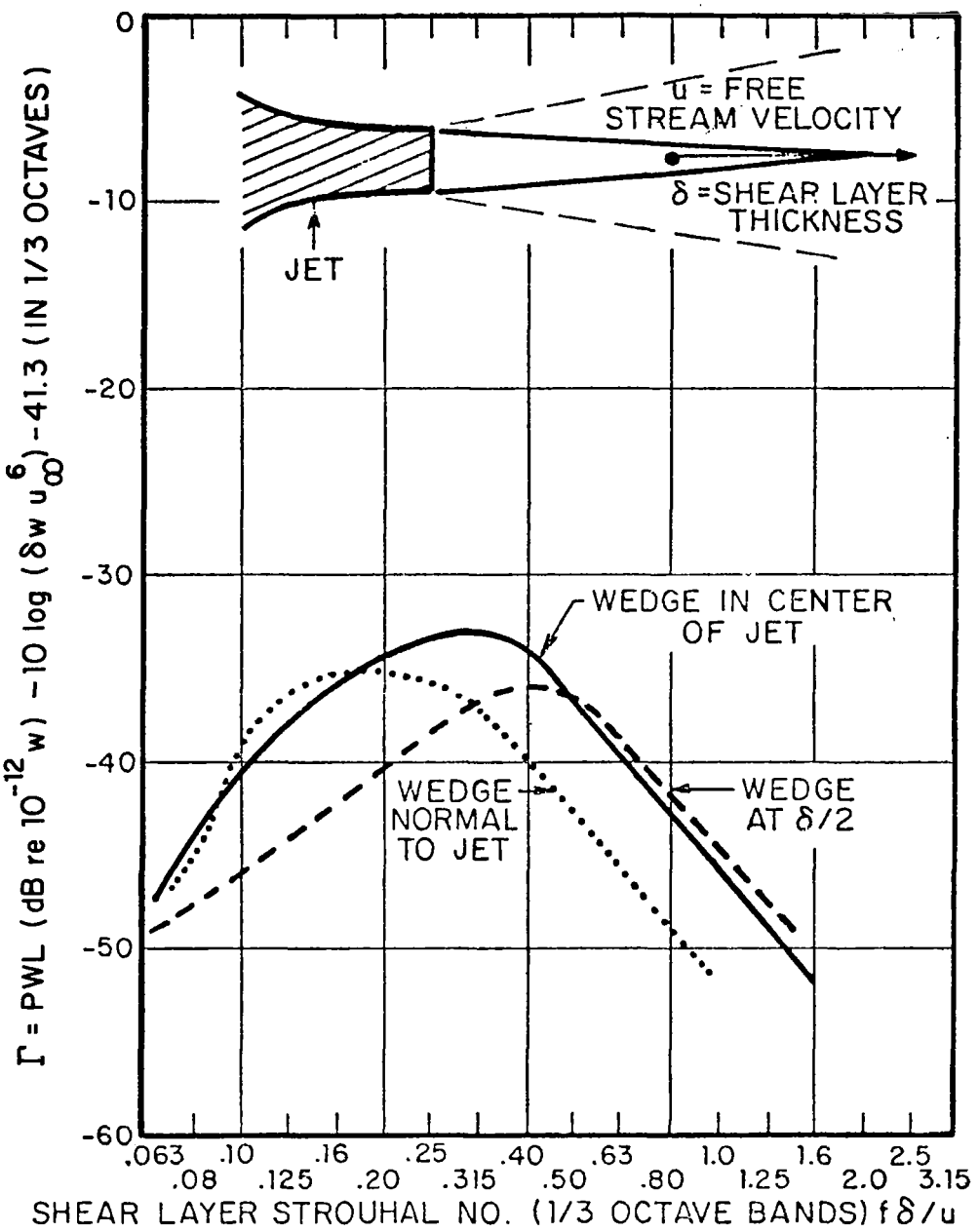

FIG. 18. RADIATED NOISE FROM AN EDGE IN A FREE SHEAR LAYER.

directivity of the source is the same as that previously reported for trailing-edge noise for thin edges. The effect of a nearby surface, such as cavity walls, floor, etc., will affect the directivity, but such effects have not yet been considered quantitatively.

Use of the spectra of Fig. 18 to predict impingement noise is justifiable, because the two orientations of the edge, normal to and aligned with the flow, represent the two surfaces which form the cavity trailing wedge. Because of the effects of flow separation, the normal orientation probably provides a good representation of the cavity rear bulkhead. Use of the data for the wedge aligned with the flow probably overestimates radiation from the surface behind the cavity. Use of these two spectra together allows the radiation to be roughly bounded with a band.

The noise due to shear layer impingement on the aft edge of the landing gear cavities was calculated using Eq. (13) and Fig. 18. As explained earlier, two situations typically occur during approach: one in which both fuselage and wing doors are open, and one in which fuselage doors are reclosed. The results shown in Fig. 19 indicate that these sources could be a dominant factor at low frequencies or at higher frequencies if the shear layer characteristics are different from those modeled.

The effects of other sources of inflow turbulence on noise radiation from the cavity trailing edge have not been estimated. These sources would include the landing gear strut when the gear is in place, and the entire assembly as the gear is being lowered. The main gear strut may be relatively unimportant, since its wake can only interact with a small fraction of the total length of the wing cavity trailing edge. In the absence of directly relevant experimental data, the effect of these sources of inflow turbulence on trailing edge noise cannot be estimated with any confidence.

Finally, the question arises as to whether the presence of the cavity can serve to amplify turbulence impingement noise through the excitation of cavity modes. For a clean rectangular cavity, which is always exposed to its own turbulent shear layer, the answer is largely contained in the semi-empirical analysis of its oscillation behavior, as discussed in the section of cavity discrete pressure oscillations. The shear layer turbulence is partially responsible for the width of tonal peaks, but is otherwise of secondary importance to the oscillation process. In fact, cavities with laminar shear layers typically oscillate more intensely, suggesting that any additional forcing due to shear layer turbulence is more than overcome by the effects of increased shear layer thickness and reduced mean velocity gradient. Similarly, introducing turbulence

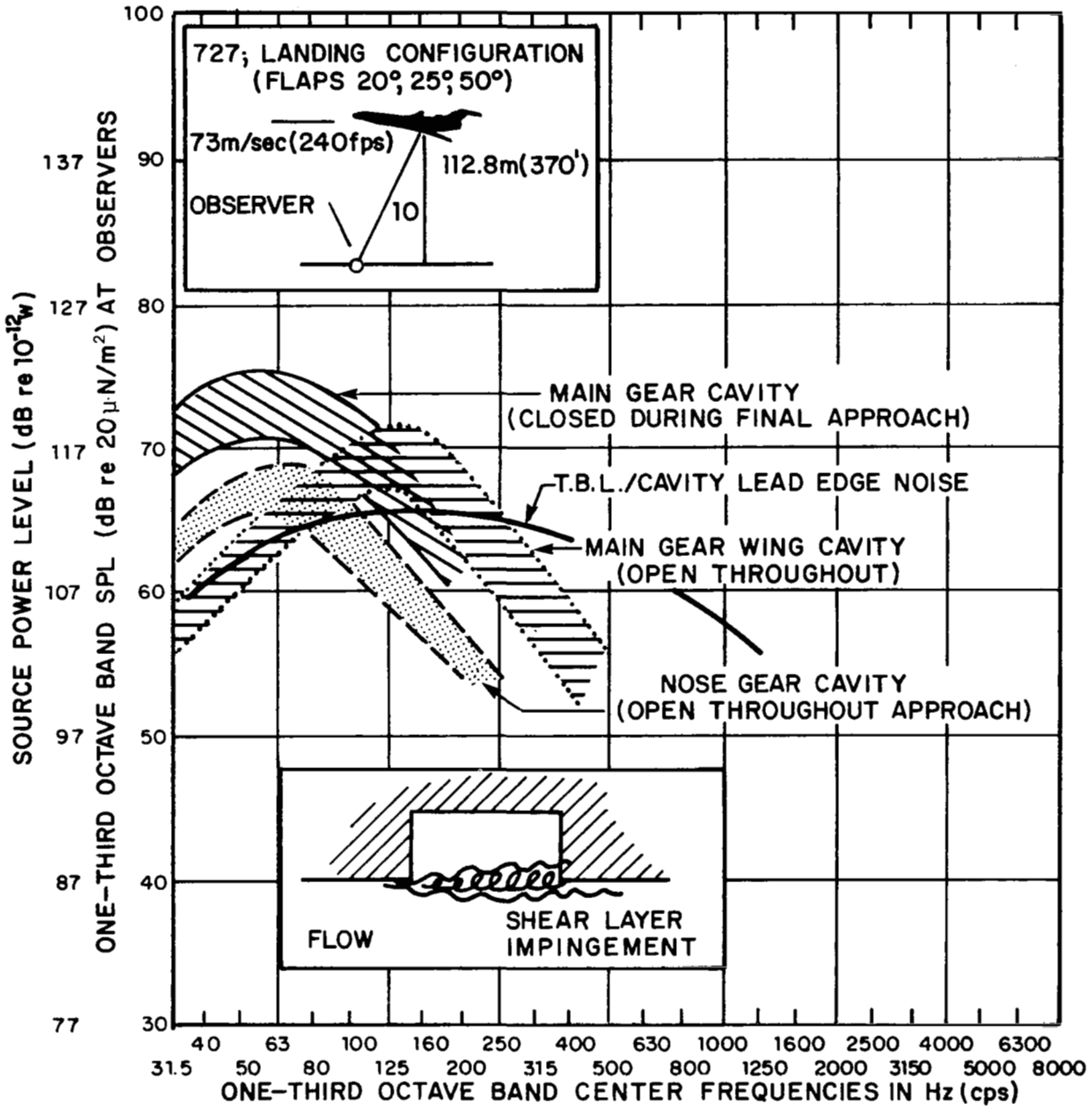

FIG. 19. ESTIMATED LANDING GEAR CAVITY EDGE NOISE SOURCES FOR A BOEING 727.

upstream of the cavity with spoilers raises the broadband and reduces the tones. We can conclude that the increase in the broadband level is directly due to changing the incident turbulence intensity rather than a coupling with the cavity dynamics.

However, when the cavity is essentially a vented enclosure rather than an open rectangular configuration, its modal characteristics are less dependent on the mean shear layer properties. In this case, it can be expected than shear layer turbulence, and particularly its impingement on the cavity trailing edge, will excite modes in the cavity enclosure and some amplification of the radiated sound may occur. Notice that the spectra of Fig. 19 fall in the same general frequency range as the vented enclosure frequencies of Table 3.

LANDING GEAR DIRECT RADIATED NOISE

Perhaps the most familiar aerodynamic noise mechanism is related to the generation of an unsteady wake by a bluff body in an airflow. Vortex shedding by cylinders at low Reynolds numbers produces narrowband sound related to the fluctuating lift and drag forces. As Reynolds number increases, the shedding becomes increasingly random and broadband noise is produced. Similarly, usually the more rough and irregular the body shape, the more broadband the resulting noise spectrum.

Fluctuations in the aerodynamic forces occur in both the direction normal to the flow, F_N, and the direction of the mean flow, F_D. The magnitude of the fluctuating forces is related to the steady state drag on the body, which is a function of Reynolds number. Values of rms normal force to steady drag are given by Jones *et al.* (1969); typically,

$$\frac{F_N}{F_{D_{SS}}} \approx 0.2 \text{ at Reynolds numbers } \frac{UD}{\nu} \approx 10^6. \qquad (14)$$

Typical values of drag fluctuations were found by Heller and Widnall (1968) to be

$$\frac{\dot{F}_D}{F_{D_{SS}}} \approx 2.3 \times 10^{-3} \ . \qquad (15)$$

The frequency, f, for the forces at a given Reynolds number is a direct proportion of the ratio of velocity to diameter (fD/U = constant). This Strouhal number, which has been studied over a wide range, is usually about 0.2 to 0.25; the bandwidth of the force fluctuations also varies with Reynolds number (Jones *et al.*, 1969).

The relationship between the spectrum of force fluctuations, Φ_F, and the spectrum of radiated sound pressure, Φ_{pa}, may be given by

$$\Phi_{pa}(r,\theta,\psi,\omega) = \frac{\Phi_F(\omega)\omega^2}{16\pi^2 r^2 c_0^2} \cos^2\theta \ , \tag{16}$$

for frequencies whose wavelengths are much longer than a dimension of the surface. The angle θ is taken from the axis of the force fluctuations. The sound power spectrum is

$$\frac{d\Pi}{d\omega} = \frac{\Phi_F(\omega)\omega^2}{12\pi\rho c^3} \tag{17}$$

For a typical aircraft, the bluff body protrusions that cause wake-related force noise are not simply shapes, as shown in Fig. 20 and Figs. 3 through 7. Notice that because of their thick flat edges, the landing gear doors are considered to behave similarly to the more blunt struts and wheels.

The difficulty in performing a prediction of the noise from struts, wheels, bluff doors, etc., is the estimation of the appropriate forces and their frequency spectrum. The gear was broken into small components, and the fluctuating lift and drag calculated for each section. Reynolds numbers based on section diameter (or, in the case of wheels, the tire width) were around 1 to 2 $\times$ 10^6. For cylinders in this range, Jones' data show that the Strouhal number of the peak normal force fluctuation is about 0.25, the rms magnitude of the normal force ranges between 0.08 to 0.12 times the steady drag, and the spectrum has a broadband character, unlike vortex shedding at lower or much higher Reynolds numbers. The overall level for each section was computed using Eq. (14) and applying Heller and Widnall's (1968) broadband spectrum (the 1/3-octave band peak occurring at the shedding Strouhal number is 15 dB below the overall level), shown in Fig. 21.

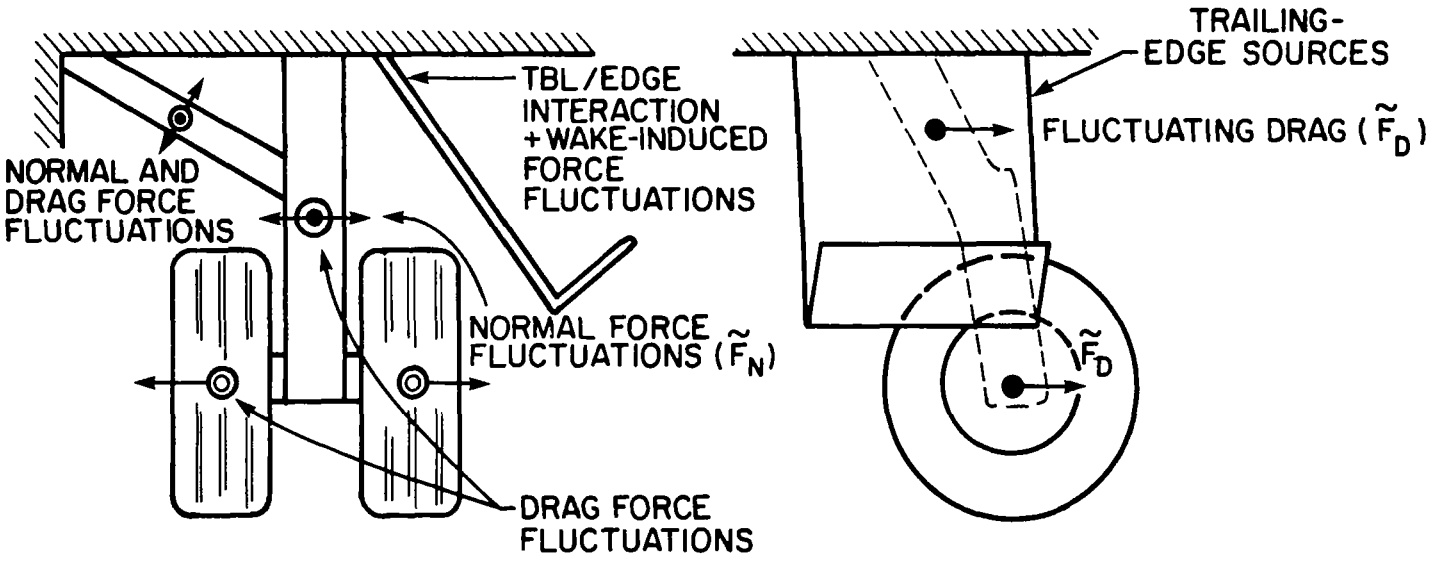

FIG. 20. LANDING GEAR DIRECT RADIATION SOURCES.

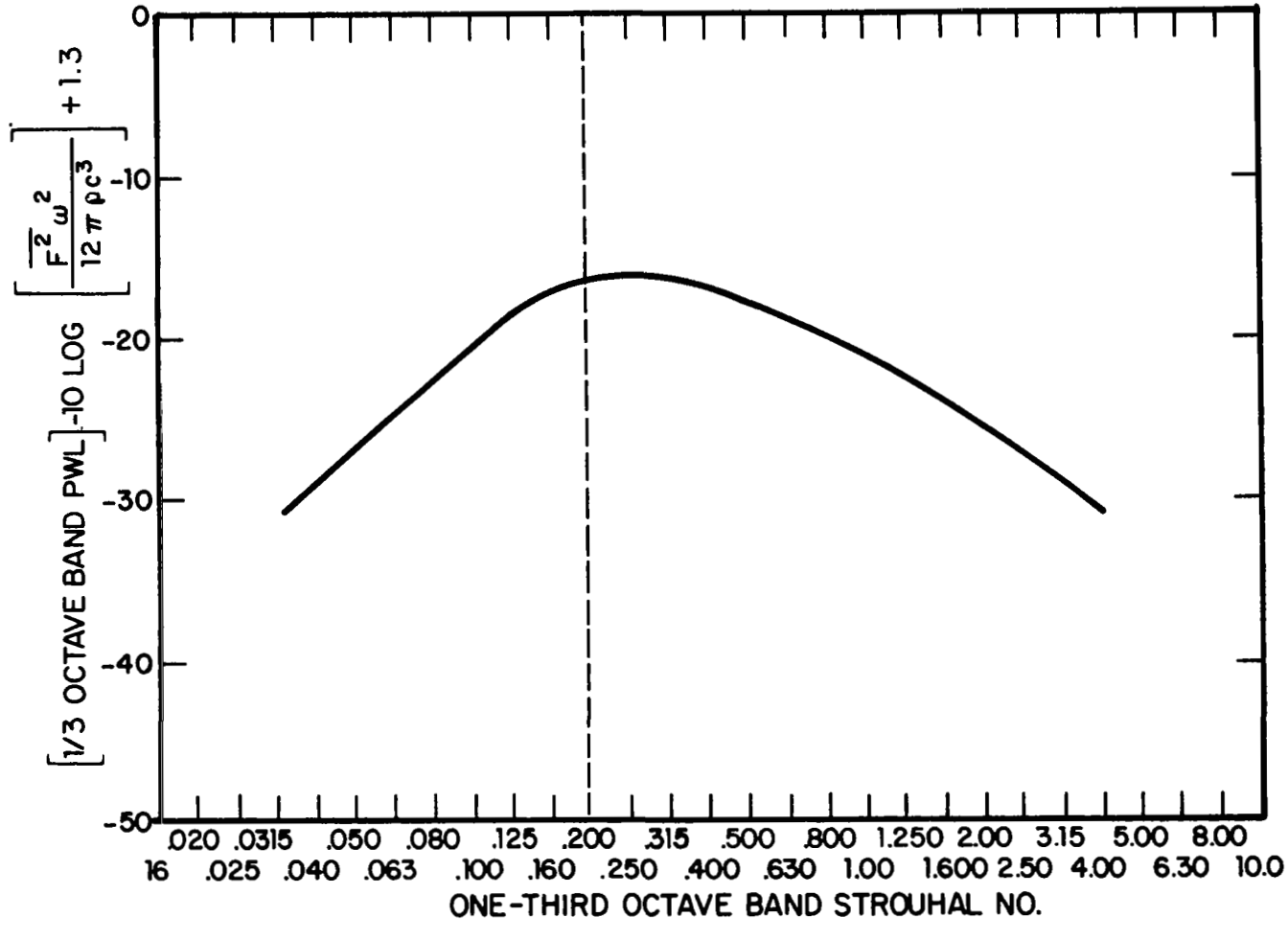

FIG. 21. SPECTRUM RELATIVE TO OVERALL LEVEL FOR NOISE FROM BLUFF BODIES.

The drag fluctuations were computed using Eq. (15) and Heller and Widnall's Strouhal spectrum centered at $fD/U = 0.4$.

The composite spectra for different components are shown in Fig. 22. The drag fluctuations contribute little to the total sound output as expected. The low-frequency area is dominated by the wheels (which were assumed to undergo flow separation at the maximum diameter point), and struts dominate the high-frequency area. The total power level dominates that of the wing edge sources at low frequencies. In considering the farfield contribution of the direct radiated sound, after-reflection effects of directivity should be carefully estimated. To obtain an estimate of the direct radiated noise (SPL) of the gears at the same ground observer point, 50 dB could be subtracted from the power levels. However, it should be recognized that because of the inhomogeneous nature of the components and the local flow around the gear, these estimates are already gross.

The cavity turbulent shear layer will impinge on the landing gear struts and braces, thereby subjecting a portion of these elements to an unsteady inflow. As a result, additional loads will be produced in the impingement region, and the vortex shedding process may be affected over the entire length of the element. If the impingement region is a relatively small portion of the element span, and if the Reynolds number is sufficiently high so that the shedding is already turbulent, these effects may not be too important. On the other hand, if the vortex shedding process was initially discrete, the addition of inflow turbulence to any portion of the strut might disrupt the discrete shedding process.

On some landing gear configurations, the wakes of some gear components may impinge on other gear components and produce unsteady loads. This interaction may occur on the in-line main struts and wheels of some large aircraft. The importance of this noise source will strongly depend on the particular landing gear geometry. Landing gear wake/landing gear interactions have not been considered in this report, and it is believed that directly relevant experimental data would be required to make a reasonable estimate of effect on radiated noise.

CAVITY AND GEAR WAKE INTERACTIONS WITH THE WING TRAILING EDGE AND FLAPS

The turbulent wakes behind the landing gear cavities and struts may induce unsteady loads on the wing trailing edge and

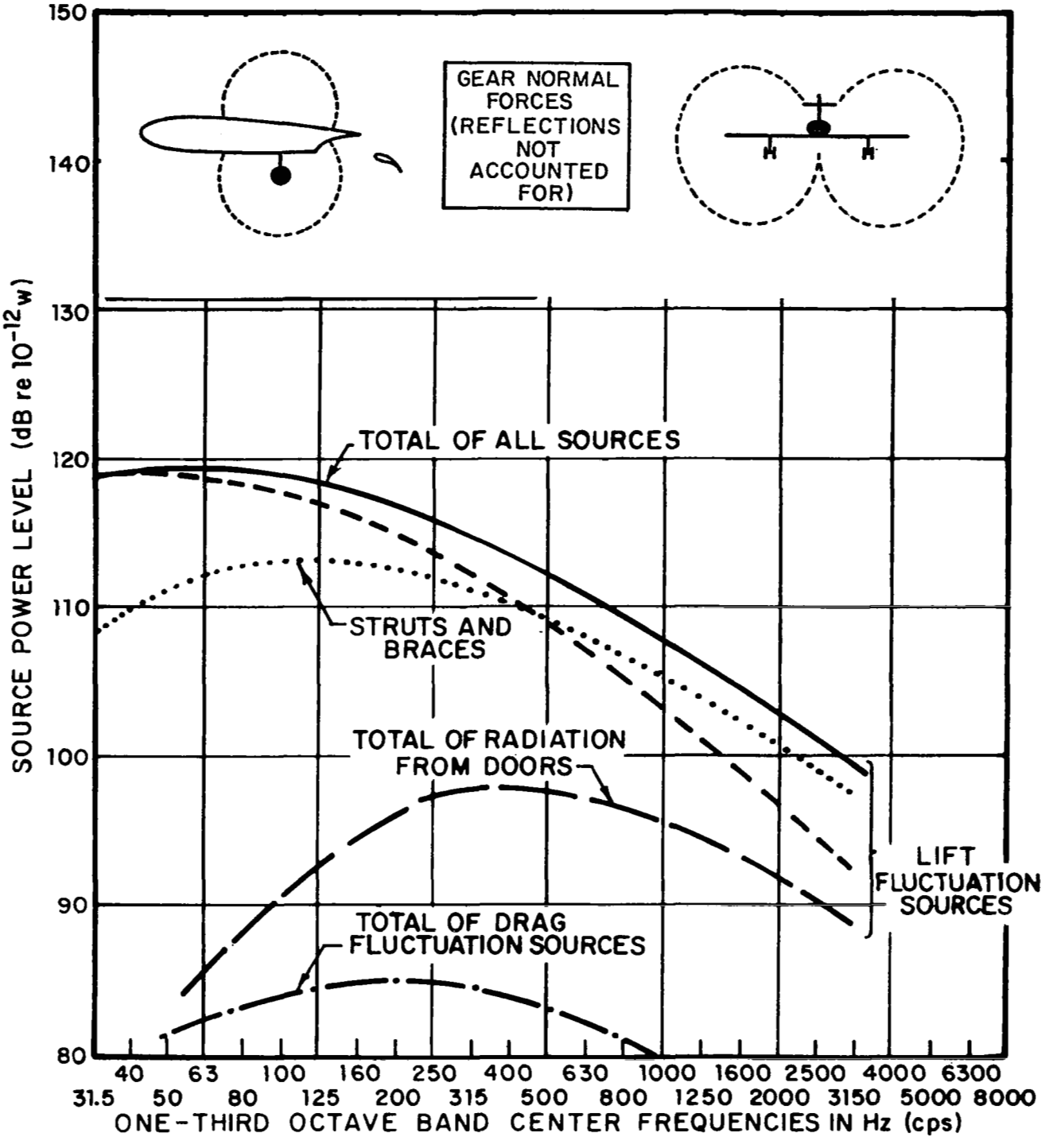

FIG. 22. LANDING GEAR DIRECT RADIATED NOISE.

the flap system. This effect is illustrated schematically in Fig. 23. These loads are produced by direct turbulence impingement and by the effect of turbulent flow over the wing and flap edges. The resulting impingement noise and edge noise will depend on the turbulence spectrum of the wakes and on the interaction geometry; these noise sources can be expected to have a dipole-like character. The wake behind the wing gear and cavity is composed of the turbulent flow from half the cavity shear layer as well as the wakes of struts, braces, and wheels. Because the cavity shear layer is adjacent to the lower surface of the wing it must inevitably interact with the wing trailing edge and flap system. The degree of interaction with the wakes of other components is less certain, and presumably depends on the flap setting.

Because of the complicated nature of this noise source, a quantitative estimate of the overall level and spectrum has not been attempted. It is believed that an experimental simulation of the wake/flap interaction flow will be required to make a reliable noise prediction. Since a very turbulent landing gear wake is expected, this interaction may prove to be an important airframe noise source.

COMPOSITE NOISE PREDICTION

The results of the previous sections can be combined with the prediction of Hayden *et al.* (1974) for the wings, flaps, and stabilizer of a Boeing 727 to obtain a composite of all noise sources during approach. The result is shown in Fig. 24 for different cavity and landing gear situations. It appears that wing, flap, and stabilizer sources control the high-frequency range, while gear direct radiated noise and shear layer impingement on the cavity aft edge dominate the low-frequency area.

The region where most of the cavity oscillation peak levels were estimated to occur is indicated by the cross-hatched box in the upper left of Fig. 24. Since these estimates are very likely high, the actual levels probably fall below the box. The indication is that cavity oscillations can be an airframe noise problem, but only if they occur for real aircraft landing gear configurations.

To estimate the level at the FAA certification point, the directivity and path effects must be considered. Figure 24 illustrates this level for the edge sources whose directivity is

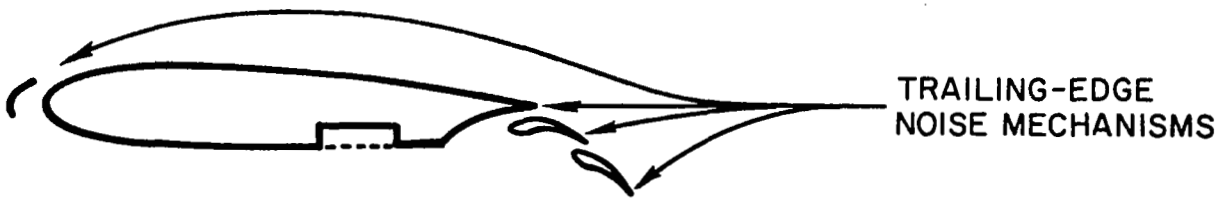

(a) "CLEAN" WING AND FLAPS

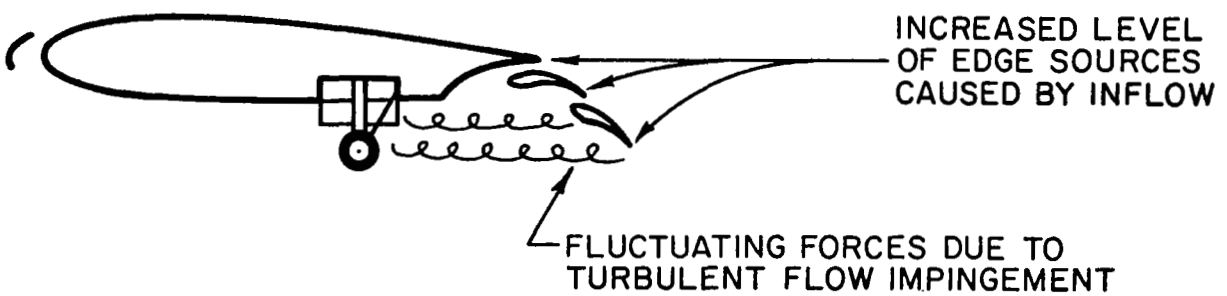

(b) WING WITH LANDING GEAR DOWN

FIG. 23. ILLUSTRATION OF POSSIBLE CAVITY AND GEAR WAKE IMPINGEMENT ON THE WING TRAILING EDGE AND FLAPS.

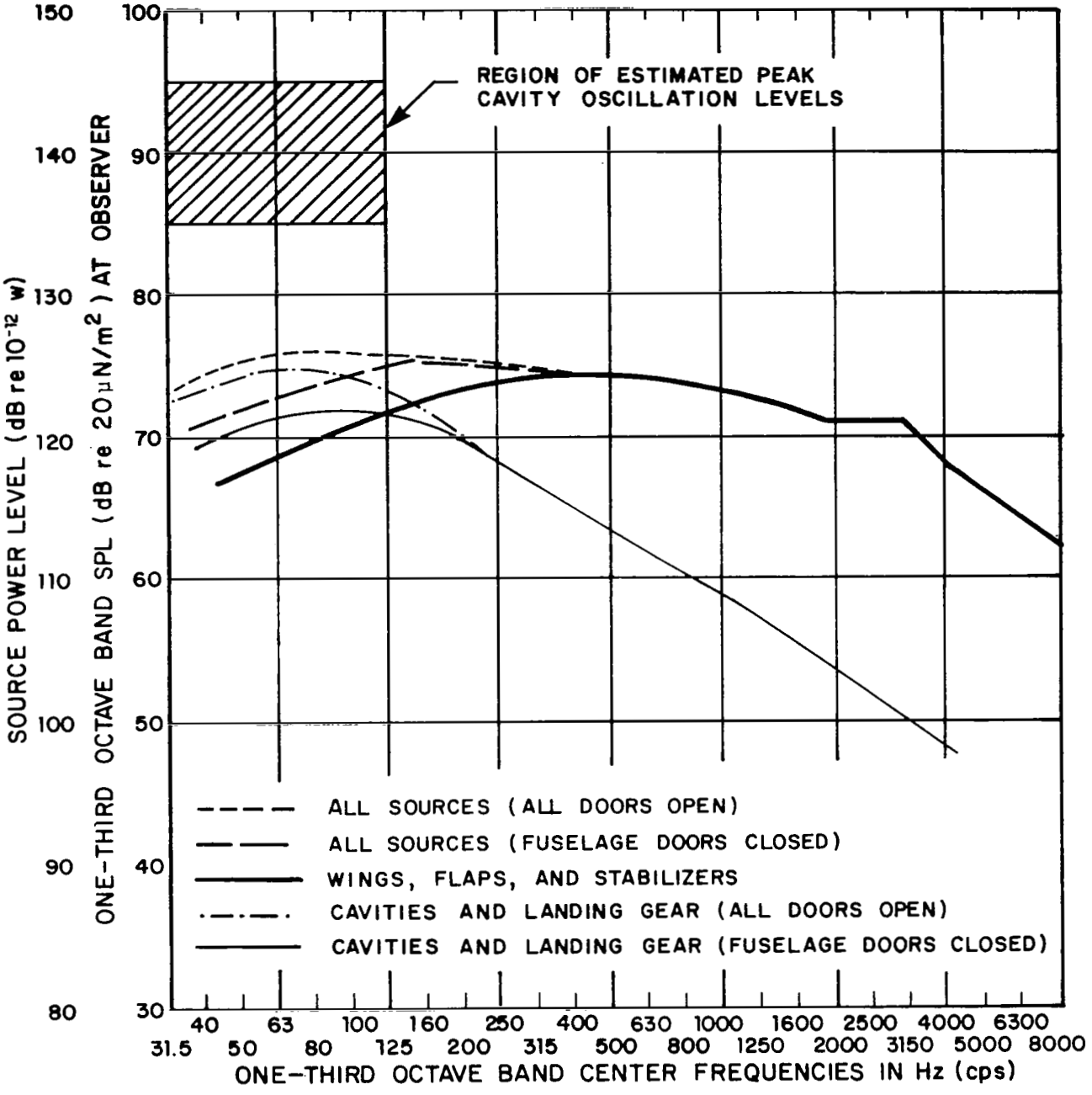

FIG. 24. COMPOSITE OF ALL SOURCES FOR THE BOEING 727, 73 m/sec (240 ft/sec), 112.8 m (370 ft) ALTITUDE.

relatively uncomplicated. It would be reasonably conservative to subtract 50 dB from the source power levels of the other sources to obtain the SPL at the observer position shown for the approach certification point (ground reflection neglected). Thus, one would expect to observe 1/3-octave band levels of 75 to 78 dB between 60 and 800 Hz, and overall levels of 88 to 91 dB for the situation modeled. The perceived noise level is approximately 97 PNdB, which is above FAR 36-10 dB for the Boeing 727.

REFERENCES

1. Hardin, J.C., Fratello, D.J., Hayden, R.E., Kadman, Y.K., and Africk, S., "Prediction of Airframe Noise," NASA TN D-7821.

2. Hayden, R.E. (1972). "Noise from Interaction of Flow with Rigid Surfaces: A Review of Current Status of Prediction Techniques," BBN Report No. 2276; also NASA CR-2126.

3. Hayden, R.E. (1972). "Fundamental Aspects of Noise Reduction from Powered Lift Devices," Invited Paper, 1973 SAE National Air Transportation Meeting, Miami, Florida.

4. Hayden, R.E., Kadman, Y.K., and Africk, S. (1974). "An Approach to Detailed Diagnostic Calculations of Airframe Noise," BBN Report No. 2791.

5. Hayden, R.E., Kadman, Y.K., and Chanaud, R.C. (1972). "A Study of the Variable Impedance Surface Concept as a Means for Reducing Noise from Jet Interaction with Deployed Lift-Augmenting Flaps," BBN Report No. 2399; also NASA CR-112166.

6. Hayden, R.E., Kadman, Y.K., Bliss, D.B., and Africk, S. (1975). "Diagnostic Calculations of Airframe-Radiated Noise," presented at the AIAA 2nd Aero-Acoustics Conference, March, Hampton, Virginia.

7. Heller, H.H., Holmes, G., and Covert, E.E. (1971). "Flow-Induced Pressure Oscillations in Shallow Cavities," *J. Sound Vib.* **18**, No. 4, 545-553.

8. Heller, H.H. and Bliss, D.B. (1974). "Aerodynamically Induced Pressure Oscillations in Cavities: Physical Mechanisms and Suppression Concepts," AFFDL-TR-74-133.

9. Heller, H.H. and Bliss, D.B. (1975). "The Physical Mechanism of Flow-Induced Pressure Fluctuations in Cavities and Concepts for Their Suppression," presented at the AIAA 2nd Aero-Acoustic Conference, March, Hampton, Virginia.

10. Heller, H.H. and Widnall, S. (1968). "Correlation of Fluctuating Forces with the Sound Radiated from Rigid Flow Spoilers," BBN Report No. 1734; also *J. Acoust. Soc. Am.* **47**(3) (1970).

11. Heller, H.H. (1974). Experimental work performed under contract to NASA Langley, presently unpublished.

12. Jones, G.W., Cincotta, J.J., and Walker, J.W. (1969). "Aerodynamic Forces on a Stationary and Oscillating Circular Cylinder at High Reynolds Numbers," NASA TR-R-300.

13. Karamacheti, K. (1955). "Acoustic Radiation from Two Dimensional Rectangular Cutouts in Aerodynamic Surfaces," NACA TN 3487.

14. Rossiter, J.E. (1966). "Wind Tunnel Experiments on the Flow Over Rectangular Cavities at Subsonic and Transonic Speeds," Royal Aircraft Establishment ARC R&M 3438.